1 Crossroads of Particle Physics and Astrophysics

Photo montage of gamma-ray sources discovered by the H.E.S.S. Cherenkov telescopes, superimposed onto an optical image of the Namibian sky.

1.1 The High-Energy Universe

Introduction

High-energy astrophysics at MPIK is primarily concerned with the study of non-thermal phenomena in the Universe using ground-based instruments to detect very-high-energy (VHE) gamma rays from the cosmos, and with the theoretical and phenomenological study of the acceleration mechanisms in cosmic sources of high-energy particles.

Particles in the VHE energy range – with energies around 10^{12} electron volts – cannot be produced as thermal radiation, like the electromagnetic radiation in most other wavelength regimes; only in the Big Bang high enough temperatures were reached for a short time. Instead, collective non-thermal mechanisms are believed to be responsible for the acceleration: charged particles continue to gain energy by diffusively returning many times into the shock front of the giant shock waves generated in supernova explosions or in the plasma jets emerging from the immediate vicinity of the massive black holes at the centers of active galaxies.

The VHE gamma rays detected on Earth are secondary products generated when the primary charged accelerated particles react with the ambient medium – either the interstellar gas or the ambient photon fields. Since the gamma rays travel on a straight path from the source to the observer, they allow imaging of sources and study of the processes in the acceleration region. The primary charged particles are deflected in galactic and intergalactic magnetic fields and either cannot reach the Earth at all – in case of sources in distant galaxies – or will only arrive after a million-year diffusive motion, where they lose all directional information concerning their origin.

High-energy astrophysics at MPIK was and continues to be characterized by a very close cooperation between experimentalists coming from a particle physics background and the more theoretically oriented astrophysicists. The following sections introduce the H.E.S.S. telescopes and the CTA next-generation project, discuss selected results from H.E.S.S., present aspects of the work of the theory groups at the institute, and conclude with results from infrared astrophysics, connected to high-energy astrophysics since it diagnoses the interaction targets.

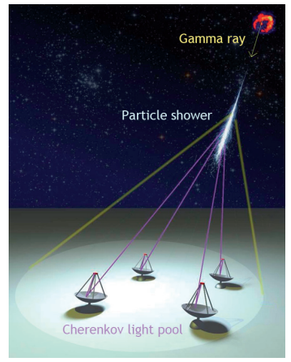

Fig. 1: Detection of primary gamma rays using the Cherenkov light from the gamma-ray induced air showers. The different views of the air shower provided by multiple telescopes allow reconstruction of the shower geometry and hence of the direction of the incident gamma ray.

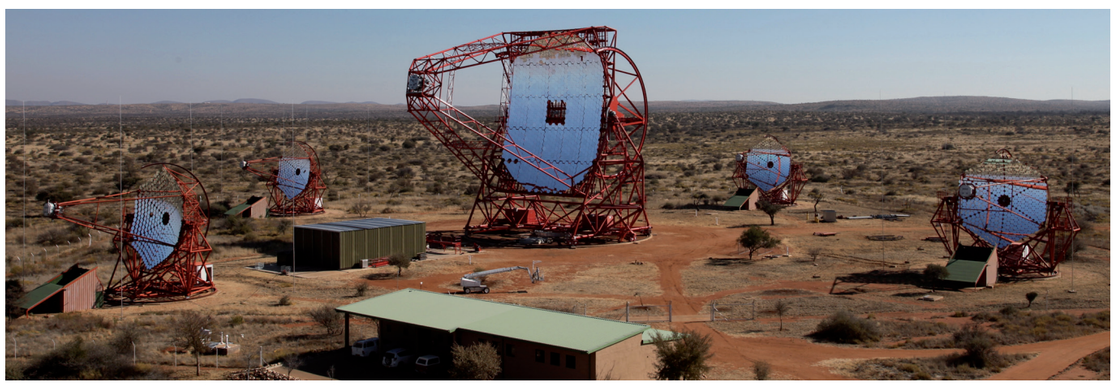

Fig. 2: The new 600 m² H.E.S.S. II telescope at the center of the H.E.S.S. telescope array.

Fig. 3: The "Big Lift": One of the most critical moments in assembling the telescope was the lifting of the dish.

Cherenkov Telescopes for Very-High-Energy Gamma-Ray Astronomy

Cherenkov telescopes have emerged as the prime instrument for ground-based astrophysics in the VHE energy range. Cherenkov telescopes detect the optical Cherenkov light produced high up in the atmosphere by high-energy particles which are generated when a primary gamma ray or cosmic ray interacts and gives rise to a cascade of secondary particles. While most of these secondary particles never reach the ground, their Cherenkov light illuminates a huge circular area of about 250 m diameter on the ground and can be detected there (Fig. 1). Cherenkov telescopes use large optical reflectors to image – in dark nights – the air shower tracks onto a matrix of photon detectors, the "camera". Compared to satellite-based instruments, which intercept the incident radiation above the atmosphere, Cherenkov telescopes have a huge detection area of $\sim 10^5$ m^2, governed by the diameter of the Cherenkov light pool. With such a large detection area it is possible to detect sources at Teraelectronvolt (TeV) energies, where the flux of gamma rays is around 10^{-11} gamma rays/cm^{2}s for the strongest sources, and around 10^{-13} gamma rays/cm^{2}s for the faintest sources detected so far.

The H.E.S.S. Telescope System and H.E.S.S. II – World's Largest Cherenkov Telescope

September 2012 marked the 10th anniversary of the inauguration of the 1st H.E.S.S. telescope, as well as the H.E.S.S. II inauguration [1]. The H.E.S.S. system of four telescopes – each with 108 m^2 reflector area and 960-pixel cameras – is operational since late 2003. In its first 10 years, H.E.S.S. has [1]

- taken 9415 hours of data, with 4234 hours in the band of the Galaxy and 5181 h in extragalactic space,
- recorded 6361 million air shower events,
- discovered over 80 new very-high-energy gamma-ray sources, among them more than 60 galactic objects and 19 extragalactic sources (see title image),

making H.E.S.S. – by the number of detected sources – the world-leading instrument in this energy range, having discovered well over half of all known VHE gamma-ray emitters.

The 600 m^2 H.E.S.S. II telescope (also referred to as CT5), located at the center of the H.E.S.S. telescope array with the telescopes CT1-CT4 (Fig. 2), was designed to improve the H.E.S.S. telescope system further, by i) expanding the energy range down to about 20 GeV for observations using CT5 alone, ii) extending the energy range for stereoscopic observations down to about 50 GeV, using coincidences between CT5 and one of CT1-CT4,

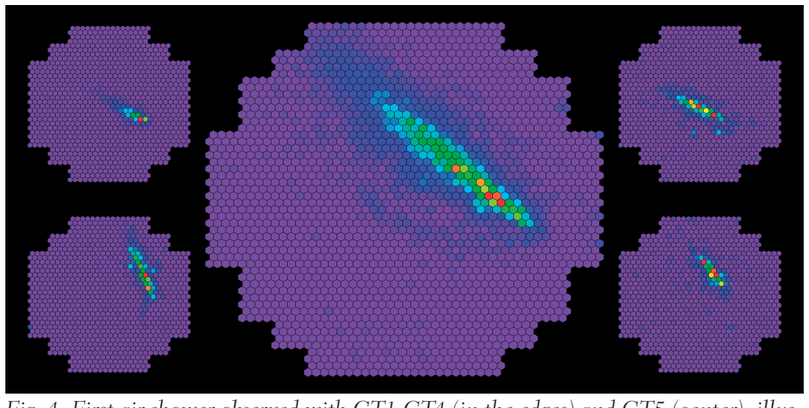

Fig. 4: First air shower observed with CT1-CT4 (in the edges) and CT5 (center), illustrating the superior images provided by CT5.

and iii) to boosting sensitivity at higher energies due to its superior imaging – with 4 times the number of pixels per unit area of sky – allowing improved angular resolution and background rejection. Construction of the telescope started in 2006. Unfortunately, problems at the company responsible for producing the 600-ton steel structure delayed the construction of CT5, and resulted in the termination of the contract by MPIK in October 2009. After a new tender process, production of the steel construction was resumed in August 2010 by a different manufacturer, who succeeded in completing the telescope structure within a very ambitious schedule of only 15 months. During the final assembly stage (Fig. 3), MPIK personnel was heavily involved in mounting precision components of the drives, bogies and bearings that were supplied directly by MPIK. After commissioning of the drive system, mirrors and their actuators, and other auxiliary systems as well as the Cherenkov camera were installed by the collaboration. Finally, on 27 of July 2012 the new telescope recorded its first images from air showers [1] (Fig. 4). In September 2012 the H.E.S.S. experiment phase II was then inaugurated by the Minister of Education of Namibia (Fig. 5).

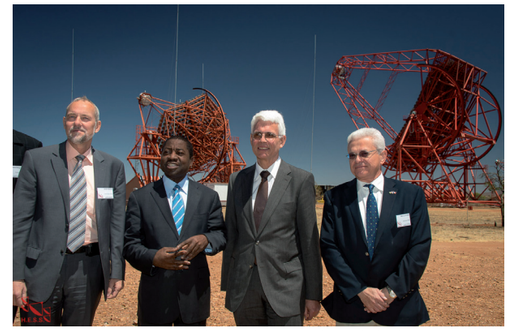

Fig. 5: German Ambassador André Scholz, Minister Abraham Iyambo, H.E.S.S. Spokesperson Werner Hofmann and French Ambassador Jean-Louis Zoël (from left) in front of one of the four H.E.S.S. I telescopes and the new H.E.S.S. II telescope.

In the following period, commissioning and characterization of the telescope and of its camera continued, such that the telescope can now be used for routine scientific operation, recording images of air showers at a rate of up to 2 kHz. In parallel to the telescopes construction, analysis software packages were adapted to reconstruct stereo events with CT5, and methods were developed to analyse very-low-energy events where only CT5 provides an image. As a first result, Fig. 6 shows the sky map from a short observation of the 'standard candle' of VHE astronomy, the Crab Nebula. A variety of other sources are already detected with CT5, and data analysis is underway.

Michael Panter, Andreas Förster, Petter Hofverberg

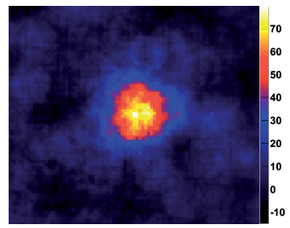

Fig. 6: The crab nebula seen by CT5. The energy threshold is significantly reduced compared to data taken with CT1-CT4.

The Cherenkov Telescope Array (CTA) Project

Based on the success of the current generation of Cherenkov telescope experiments (H.E.S.S., MAGIC and VERITAS), scientists have joined to work towards the construction of the next-generation instrument: the Cherenkov Telescope Array (CTA). The aim of the CTA project is the construction of an observatory for ground-based gamma-ray astronomy with a sensitivity of a factor 10 better than the current-generation instruments. Besides the improved sensitivity with respect to current instruments, CTA will provide larger energy coverage of over 4 decades from a few 10 GeV to several 100 TeV. Together with its better angular resolution reaching into the few-arcmin regime and its larger field of view, CTA will be able to resolve the morphology of extended astrophysical objects on fine angular scales. At the same time it will be a highly sensitive instrument for surveys of the sky as well as for the search for point-like sources. Full sky coverage will be achieved through the installation of two arrays, one in the southern hemisphere, providing full energy coverage, and a northern array with emphasis on the low-energy instrumentation. To cover the whole energy range and to provide the required performance parameters in a cost effective way, CTA arrays will consist of up to about 100 Cherenkov telescopes of different classes with dish diameters of approximately 4, 12 and 23 m, distributed over an area of about 5 km^2 in the southern array and about 1 km^2 in the northern array (see Fig. 7). The total investment cost for CTA is expected to be of the order of 200 M€. The project was initiated in 2006 by members of the H.E.S.S. and MAGIC experiments. Meanwhile, the collaboration consists of more than 1100 members from 173 institutes in 28 countries on 5 continents. CTA is included in the ESFRI roadmap for European Research Infrastructures and is highly ranked in the national roadmaps of astroparticle physics and of astronomy. After a four year design study, in 2010/11 CTA has entered its preparatory phase, which is coordinated by MPIK and supported through the 7th framework programme of the European Commission. The goal of the CTA preparatory phase is to bring CTA to production readiness by the end of 2014. Current work is therefore mainly concerned with the technical design and prototyping of telescopes, software and auxiliary systems, with the implementation of proper project management, as well as with the preparation of the legal, financial and

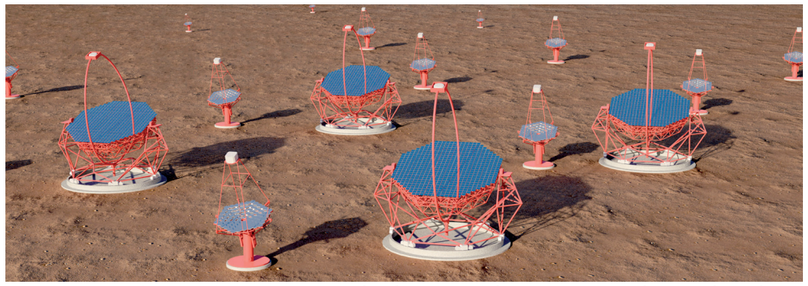

Fig. 7: An artist's view of a CTA array with telescopes of the 4 m, 12 m and 23 m class, distributed over an area of several km².

administrative structures for the CTA observatory. A preliminary technical design report for CTA has been released in late 2013. A board of representatives of funding agencies has been installed to monitor and to steer the project. In 2012 a "Declaration of Intent" towards implementation of CTA has been signed by the representatives of the funding agencies. MPIK is playing a leading role, with Werner Hofmann as spokesperson of CTA, and several institute members in coordinating functions of CTA work packages. Key development activities, like the optimization and verification of array layouts through extensive Monte Carlo simulations as well as a camera development (FlashCam) at the technological forefront are driven by MPIK. Members of MPIK are also involved in the definition of key science cases for CTA.

Konrad Bernlöhr, Andreas Förster, German Hermann

FlashCam: a Fully Digital Camera for the CTA Telescopes

FlashCam is a camera development project for the Cherenkov Telescope Array (CTA). FlashCam has been initiated by the MPIK, and is carried out in cooperation with partner groups from Germany, Switzerland, Austria and Poland. In contrast to "classical" Cherenkov cameras, as installed in current-generation telescopes, the FlashCam concept follows a fully digital approach for the signal processing, using commercially available microchips as produced for the growing digital communication market. Besides the mechanical structure, the key building blocks of such a camera are the photon detector plane (PDP), the readout electronics (ROS) and the data acquisition system (DAQ) with the camera server CPU (see Fig. 8). This functional division provides a high degree of flexibility e. g. in the choice of the photo detectors, or in the detailed layout of the camera. For the mid-size (12 m dish diameter) CTA telescopes, the 1764 pixel photon detector plane consists of 147 PDP-modules, each with 12 photomultiplier tubes (PMT). Each module includes high voltage supplies, pre-amplifiers and a microcontroller for control, monitoring and safety functions. The analogue signals from the pixels are transmitted through standard CAT5 cables to the readout electronics. The custom-developed readout electronics of the camera uses fast analogue to digital converters (FADC) that digitize the incoming signals continuously with

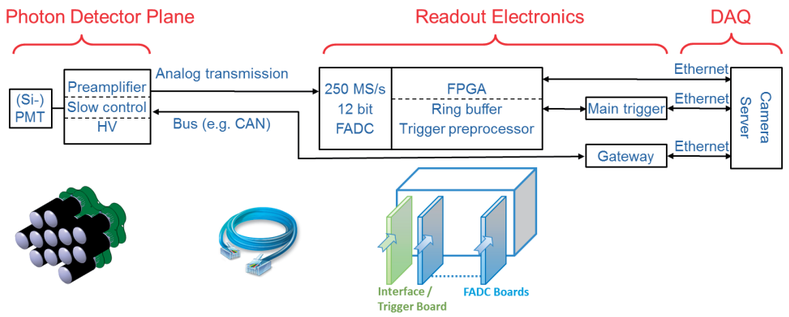

Fig. 8: Basic building blocks of a FlashCam camera.

a sampling frequency of 250 MSamples/s and an amplitude range of 12 Bit. The digitized signals of 24 channels per electronics board are then buffered and digitally processed in a field programmable gate array (FPGA), in order to compute amplitude and time information of the pixel. The key point of this concept is to perform all signal processing based on digitized information. In particular, the trigger decision to store an image is computed in the camera solely from the digitized signals. Depending on configuration, the total continuous data traffic which is processed within the camera electronics amounts up to more than 2 TBit/s. Upon a trigger, the digital image information is then sent to the camera server of the data acquisition system (DAQ), using standard ethernet components. A special software library based on the raw ethernet protocol has been developed. Tests have demonstrated that FlashCam will be able to acquire more than 30 000 images per second without any dead-time, more than a factor of 10 faster than current cameras. As of end of 2013, the FlashCam team successfully operates a 144 pixel mini-camera with all basic building blocks to verify the performance parameters of the implementation. It is planned to build in 2014 a full-sized camera prototype, to verify performance and camera characteristics on the system level.

Christian Bauer, German Hermann, Quirin Weitzel

Science results from H.E.S.S.

The following examples illustrate the range of recent science results obtained using the four H.E.S.S. telescopes: from surveys and investigation of Galactic sources, detection of sources in nearby galaxies and of starburst galaxies, to the study of the cosmologic extragalactic background light using gamma rays from AGN, and the search for signatures of Dark Matter annihilation. A final section addresses the development of improved methods for image analysis.

The H.E.S.S. Galactic plane survey: H.E.S.S. has undertaken the first comprehensive survey of the inner Galaxy in very-high-energy (VHE) gamma rays (H.E.S.S. Galactic Plane Survey, HGPS). The data set of the HGPS comprises 2800 hours of high-quality data, taken in the years 2004 to 2013. The sensitivity for the detection of point-like sources is at the level of 2% Crab or better in the HGPS region. This survey has led to the discovery of an unexpectedly large and diverse population of over 60 sources of TeV gamma rays within its current range of $l = 250$ to 65 degrees in longitude and $|b| < 3.5$ degrees in latitude (title picture and Fig. 9). From the HGPS currently a catalogue for VHE gamma-ray sources is being constructed. The main challenge for the construction of the catalogue is the fact that most VHE gamma-ray sources are extended and several of them overlap. This catalogue will enable for the first time to study the populations of Galactic VHE gamma-ray emitters.

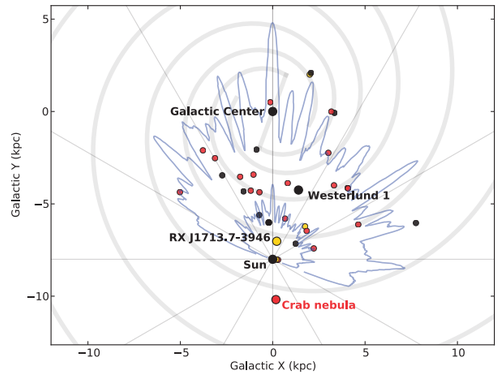

Fig. 9: Location of sources with known distance in the Galaxy. The H.E.S.S. detection horizons for 1% and 10% of the Crab Nebula luminosity above 1 TeV fare depicted by the blue curves. SNRs are shown in yellow, PWNs in red and all other sources in black. Also indicated is the spiral structure of the Galaxy.

The population of TeV gamma-ray emitters is dominated by the pulsar wind nebula (PWN) and supernova remnant (SNR) source classes, although nearly a third of the sources remain unidentified or ambiguous. One of the important results of the HGPS is the discovery of a significant number of evolved PWNe. Some of them have only faint counterparts in other wavelengths and have previously not been found in other energy bands. The observed population of PWNe of different ages also enables to study the evolution of these objects. Probing the VHE gamma-ray emission from SNRs is another important population study on the basis of HGPS data. SNRs are the proposed sources of cosmic rays and should therefore be emitters of VHE gamma radiation, as a tracer of these highly energetic particles. Positions of SNRs, known from other wavelengths, are checked for gamma-ray emission in the HGPS field. It appears that the number of detected SNRs is consistent with the picture that SNRs are the main source of cosmic rays. HGPS data are also used to search for diffuse VHE gamma-ray emission from the Galaxy. Significant emission is detected outside the source regions, peaking at the galactic plane. The nature of this diffuse emission is not known to date. Most likely it represents a superposition of unresolved sources, of truly diffuse emission

generated by the nucleonic cosmic rays interacting with the interstellar medium and of VHE photons generated by the up-scattering of low-energy photons by highly energetic electrons in the vicinity of Galactic electron accelerators.

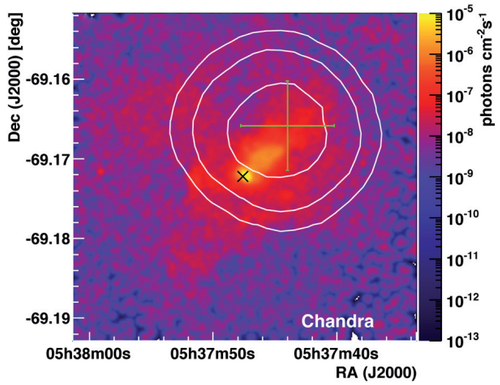

Fig. 10: The pulsar wind nebula N 157B in the LMC, viewed in X-rays in the energy band from 0.8 keV to 8 keV. The white contour lines denote regions of 68%, 95%, and 99% confidence for the position of the gamma-ray source HESS J0537–691.

Discovery of gamma-ray emission from the extragalactic pulsar wind nebula N 157B [2]: Pulsars with high spin-down luminosity power electron-positron nebulae (Pulsar Wind Nebulae, PWN) that emit gamma rays up to energies of several tens of TeV. In the H.E.S.S. galactic plane survey it has been found that PWN likely comprise the most numerous type of Galactic sources. So far only PWNe inside the Galaxy have been detected in gamma-rays. H.E.S.S. has observed the Large Magellanic Cloud (LMC) – a satellite galaxy to the Milky Way – for 46 hours. In this exposure the PWN N 157B, the first object belonging to a Galactic source type in an external galaxy, has been detected (Fig. 10). N 157B is associated with PSR J0537-6910, which is the pulsar with the highest known spin-down luminosity. A model of the wide-band emission of N 157B shows that an energy of about 4×10^{49} erg is stored in electrons and positrons in the PWN. The detection of a PWN at such large distance is possible due to the pulsar's favorable spin-down luminosity and a bright infrared photon-field serving as an inverse-Compton-scattering target for accelerated leptons. From the energy accumulated in PWN electrons, the pulsar's birth period is estimated to be shorter than 10 ms, among the shortest birth periods deduced so far.

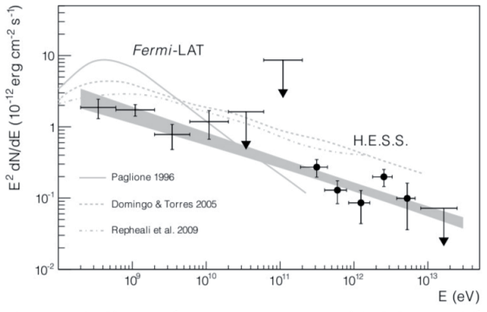

Fig. 11: Differential energy spectrum of NGC 253. The data can be described by a simple power-law over the entire energy range (shaded band). Model calculations are shown for comparison.

Spectral analysis and interpretation of the gamma-ray emission from the starburst galaxy NGC 253 [3]: Starburst galaxies exhibit in localized regions an enhanced rate of supernovae, remnants of which are believed to accelerate cosmic rays. In 2009, H.E.S.S. has indeed detected the starburst galaxy NGC 253 in gamma rays, as tracers of cosmic rays. The gamma-ray spectrum provides information on the propagation of cosmic rays in starburst galaxies and the radiation mechanism. An enlarged H.E.S.S. dataset and data of the energy range below 100 GeV from the FERMI satellite were analyzed to study the gamma-ray spectrum of NGC 253 over a wide range from 200 MeV to 5 TeV. No evidence for a spectral break or turnover is found over the dynamic range of both the FERMI-LAT instrument and the H.E.S.S. experiment: a combined fit of a power law to the gamma-ray data results in a differential photon index $\Gamma = 2.34 \pm 0.03$, see Fig. 11. The smooth alignment between the spectra over this entire energy domain suggests that the same gamma-ray production mechanism and cosmic-ray transport processes dominate in the entire energy range. Data are consistent with a scenario where cosmic ray protons and nuclei, accelerated by the numerous supernova remnants in the starburst region, produce gamma radiation by inelastic collisions with the dense interstellar medium in the same region. The gamma-ray observations indicate that at least about 20% of the energy of the cosmic rays is channeled into gamma-ray production. The rest of the cosmic rays are most likely removed from the starburst region by an energy-independent advection process.

Measurement of the extragalactic background light imprint on the spectra of the brightest blazars observed with H.E.S.S. [4]: The Universe is filled with optical to infrared photons (Extragalactic Background Light, EBL) originating from the combined radiation from all stars in the optical and from dust-reprocessed starlight in the infrared. VHE gamma-rays interact with optical-infrared photons via electron-positron pair production, resulting in an attenuated flux that is detected on Earth from extragalactic sources. The attenuation by the EBL is expected to leave a unique, redshift-dependent and energy-dependent imprint on the VHE spectra. This signature is searched by fitting the spectra of the brightest extragalactic blazars detected by H.E.S.S. with a maximum likelihood method, leaving the parameters of the intrinsic spectra free. The originality and the strength of the technique lie in the joint fit of the EBL optical depth and of the intrinsic spectra of the sources, fully accounting for intrinsic spectral curvature. This derivation of the EBL optical depth with H.E.S.S. data does not rely on constraints on the intrinsic spectrum from

assumptions about the acceleration mechanism and results in a measurement of the optical depth, compared to the upper limits derived in previous studies. Analysis of a total of $\sim 10^5$ gamma-ray events enables the detection of an EBL signature at the 8.8 std. dev. level and constitutes the first measurement of the EBL optical depth using VHE gamma rays. The EBL flux density is constrained over almost two decades of wavelength (0.30-17 μm) and the peak value at 1.4 μm is derived as $15 \pm 2\,(\text{stat}) \pm 3\,(\text{sys})$ nW/m^{2}sr, in the range predicted by models of cosmological star formation.

Search for photon-line-like signatures from Dark Matter annihilation with H.E.S.S. [5]: It is generally believed that the majority of the matter in the Universe is non-baryonic and only weakly interacts with ordinary matter – Dark Matter (DM). Gamma-ray line signatures can be expected in the VHE domain due to self-annihilation or decay of DM particles in space. Such a signal would be readily distinguishable from astrophysical gamma-ray sources that in most cases produce continuous spectra that span over several orders of magnitude in energy. Using data collected with H.E.S.S., upper limits on both continuum DM-emission and line-like emission were obtained. The search for line-like annihilation features covers the energy range from 500 GeV to 25 TeV, complementing recent limits obtained with the Fermi-LAT instrument at lower energies. No statistically significant signal could be found; line limits are illustrated in Fig. 12. For a DM particle mass of 1 TeV, limits on the velocity-averaged DM annihilation cross section reach 10^{-27} cm^{3}s^{-1}, for the Einasto parametrization of the Galactic DM halo density profile.

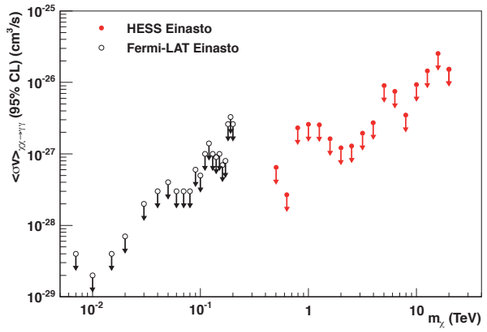

Fig. 12: Limits on the velocity-weighted cross section for DM annihilation into two photons calculated from the flux limits for the central Galactic halo region (red arrows with full data points). Limits obtained by Fermi-LAT are shown for comparison.

Image analysis: A new image template based analysis for air Cherenkov telescopes: When analysing data taken with atmospheric Cherenkov telescopes (such as the H.E.S.S. array) one must use the images of the gamma-ray induced air showers to reconstruct the direction and energy of the original gamma-ray photon. Typically this reconstruction is performed using simple "Hillas" parameterisations of the shower images. The ImPACT analysis (Image Pixelwise fit for Atmospheric Cherenkov Telescopes) is a new reconstruction method, designed to include more information of the air shower images in the reconstruction procedure. Rather than simply parameterising the camera images, ImPACT instead uses the full camera images, comparing them with a library of expected image templates produced using detailed Monte Carlo simulations. A minimisation procedure is then performed allowing the best fit direction and energy of the gamma-ray event to be determined.

This improved analysis technique provides significant improvements in performance over the traditional analysis scheme. Fig. 13 shows the angular resolution of the ImPACT method (expressed as the 68% event containment radius from a point-like source) as a function of simulated event energy. ImPACT provides around a 40% improvement in angular resolution over the traditional Hillas method, allowing the H.E.S.S. array to be more sensitive to point-like sources or allow study of extended sources in significantly more detail.

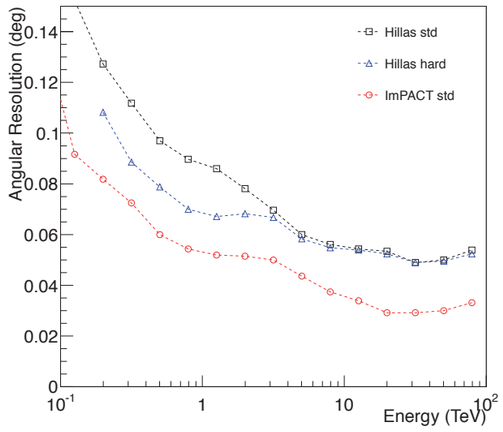

Fig. 13: Improvement on the angular resolution with the new analysis method (red) with respect to standard Hillas analysis (black, blue).

Wilfried Domainko

Theory of Radiation Processes

High-energy radiation processes in different astrophysical environments have always been in the focus of MPIK astrophysics theory research. In this regard, several interesting results have been obtained over the recent three years.

Synchro-curvature radiation of charged particles in very strong magnetic fields: Relativistic particles in strong curved magnetic fields can radiate in a regime quite

different from the standard synchrotron or curvature modes. In this regime, the radiation varies with the frequency of gyration. Because of this effect, the time-averaged spectrum of radiation detected by an observer becomes different from the energy spectra formed in the synchrotron and curvature regimes of radiation. The variability of radiation in the curved magnetic field is always present due to the time-dependence of the curvature of the trajectory, but it can be neglected in the standard curvature and synchrotron regimes. However, in the transition between these regimes, the variability starts to play a key role in the formation of the intermediate synchro-curvature radiation. To describe the particle trajectory, which has the form of a spiral wound around the drift trajectory, a Hamiltonian formalism has been invoked. It was shown that the passage to two limiting (synchrotron and curvature) cases is essentially determined by the relation between the pitch angle and the drift velocity. The curvature regime corresponds to the motion strictly along the drift trajectory. The numerical calculations with inclusion of energy losses of particles confirmed the basic conclusions from the simplified analytical treatment of the problem, and allowed to study the intermediate regime for different initial pitch angles. In particular, it was found that even tiny initial angles can result in spectra significantly different from the spectra of the synchrotron and curvature components of radiation.

Radiation of relativistic electrons in highly turbulent magnetic field: In a small-scale highly turbulent medium, when the nonrelativistic Larmor radius $R_L = mc^2/eB$ exceeds the correlation length λ of the magnetic field, the magnetic bremsstrahlung of charged relativistic particles unavoidably proceeds in the so-called jitter radiation regime. The cooling timescale of parent particles is identical to the synchrotron cooling time, thus this radiation regime can be produced with very high efficiency in different astrophysical sources characterized by high turbulence. The jitter radiation has distinct spectral features shifted toward high energies, compared to synchrotron radiation. This effect makes the jitter mechanism an attractive broad-band gamma-ray production channel, which, in highly magnetized and turbulent environments, can compete or even dominates over other high-energy radiation mechanisms. Within the framework of perturbation theory, a novel study of the spectral properties of the jitter radiation has been performed. A general expression for the spectral power of radiation in a rather compact and convenient analytical form has been derived, which can be used in detailed numerical treatments of the problem.

Study of radiation features produced at the inverse Compton scattering: The inverse Compton (IC) scattering of relativistic electrons is one of the major gamma-ray production mechanisms in different astrophysical environments. Although this process has been comprehensively studied in the past, the details of spectral features of the IC scattering are of great interest for interpretation of data obtained recently in the GeV and TeV gamma-ray bands. A variety of studies have thus been performed regarding different aspects of the formation of the IC emission. In particular, the spectral shape of the IC radiation in the Thomson and the Klein-Nishina regime in the energy band corresponding to the cut-off region of the distribution of the parent electrons has been analyzed. Simple analytical expressions for the spectrum close to the maximum cut-off region have been derived, which provide a direct link between the distribution of parent electrons and the up-scattered gamma-ray spectrum. Also, the profiles of the gamma-ray line like features of radiation produced by mono-energetic electrons have been investigated, showing that in the deep Klein-Nishina regime this mechanism can produce very sharp line feature with a width as narrow as $\Delta E/E \leq 0.2$. Such a scenario could be realized at the Comptonization of a cold ultra-relativistic pulsar wind, and should be taken into account in the searches for characteristic gamma-ray line like emission from Dark Matter as an alternative mechanism of producing sharp gamma-ray line features at very high energies.

The beaming pattern of External Compton Emission from relativistic outflows: The beaming pattern of radiation emitted by a relativistically moving source like jets in microquasars, AGN and GRBs, is a key issue for a proper understanding of acceleration and radiation processes in these objects. A formalism based on a strict solution of the photon transfer equation has thus been introduced to study the beaming patterns for the emission produced by electrons accelerated in the jet and up-scattering photons of low-energy radiation fields of external origin (the so-called External Compton scenario). The formalism allows one to treat non-stationary, non-homogeneous and anisotropic distributions of electrons, but assuming homogeneous, isotropic and non-variable target photon fields. The results demonstrated the non-negligible impact of the anisotropy in the electron distribution on angular and spectral characteristics of the External Compton component of radiation.

Nuclear gamma-radiation of very hot plasmas at temperatures kT>1 MeV: The importance of nuclear reactions in low-density astrophysical plasmas with ion temperatures exceeding 1 MeV has been recognized for almost thirty years ago. However, the lack of comprehensive data banks of relevant nuclear reactions and the limited computational power have not previously allowed detailed theoretical studies. Recent developments in these areas make it timely to conduct comprehensive studies on the nuclear properties of very hot plasmas formed around compact relativistic objects such as black holes and neutron stars. Such studies are of great interest in the context of scientific programs of future low-energy cosmic ray-ray spectrometry. A large nuclear network relevant for temperatures exceeding 1 MeV has thus been built using the publicly available code TALYS and the evolution of the chemical compositions and the accompanying prompt gamma-ray emission has been studied for such high-temperature plasmas. Results on the abundances of light elements D, T, ^{3}He, ^{4}He, ^{6}Li, ^{7}Li, ^{9}Be, ^{10}B, ^{11}B have been presented and their implications for the astrophysical abundances of these elements discussed. In addition, the gamma-ray emissivity due to the capture of neutrons by protons, p-n bremsstrahlung, and gamma-rays from decays of neutral pions produced at pp-interactions in different regimes of accretion flows has been investigated.

Felix Aharonian

Supernova Remnants and the Origin of Cosmic Rays

Diffusive shock acceleration in young supernova remnants (SNR) is the most widely accepted scenario for the acceleration of cosmic rays (CR) up to at least 10^{15} eV (PeV), the so-called knee. There is, however, no general consensus on the maximum acceleration energy achieved in the process and, up to now, no observational evidence for SNR sources capable of accelerating CRs in the Galaxy up to very high energies.

Research at MPIK has explored the processes responsible for the acceleration of particles and the broad-band radiation in the young SNR Cas A using a new code which is designed for a detailed treatment of the diffusive shock acceleration of particles in nonlinear regime, including both the forward and reverse shocks. The model is based on spherically symmetric hydrodynamic equations complemented with transport equations for relativistic particles. The available multi-wavelength observations in the radio, X-ray and gamma-ray bands can be best explained by invoking particle acceleration by both forward and reversed shocks. The acceleration efficiency in this source, despite previous claims, should be very high, with 25% of the explosion energy already converted to cosmic protons and nuclei. What concerns the electronic component, the decays of radioactive nuclei related to ^{44}Ti and ^{56}Ni ejected during supernova explosions can provide a vast pool of mildly relativistic positrons and electrons which are further accelerated to ultra-relativistic energies by the reverse and forward shocks. This interesting link between two independent processes – radioactivity and particle acceleration – can be a clue for the solution of the well-known theoretical problem of electron injection in SNRs. In the case of the brightest radio source Cas A, radioactivity can in fact supply the required 10^{48} erg in electrons (and positrons) for the interpretation of observational data provided that they are stochastically pre-accelerated in the upstream regions of the forward and reverse shocks.

Once released by their sources, cosmic rays diffuse in the interstellar medium, and finally escape from the Galaxy. The transport of cosmic rays in the Galaxy is the main obstacle to pinpoint the origin of cosmic rays. Gamma-rays are produced in cosmic-ray interactions with the interstellar medium and in inverse Compton scattering on cosmic photon fields. The diffuse gamma-ray emission from the Galactic disk can thus provide the spectrum and flux of cosmic rays in the Galaxy and help understanding how cosmic rays diffuse in the Galaxy. While a thorough investigation of this diffuse emission at TeV energies with current instruments is still difficult, recent HEAT studies have investigated the promising impact of the future CTA instrument on this issue.

The GeV emission of ten nearby giant molecular clouds belonging to the Gould Belt, detected with the Fermi Large Area Telescope (LAT), was investigated in order to infer the energy distributions of CRs in these clouds. Remarkably, both the derived spectral indices and the absolute fluxes of CR protons in the energy interval 10 - 100 GeV are in good agreement with the recent direct measurements of local CRs by the PAMELA experiment. This is a strong evidence for a quite homogeneous distribution of CRs, at least within

several hundred parsecs of the Local Galaxy. Combined with the well established energy-dependent time of escape of CRs from the Galaxy, the measured spectrum implies a CRs spectral index of the (acceleration) source of $\sim E^{-2.3}$.

Sabrina Casanova, Felix Aharonian

Another Galactic Centre Mystery Uncovered

In 2010, NASA announced the startling discovery by its orbiting gamma-ray telescope, Fermi, of two enormous gamma-ray emission structures that hang like lightglobes above and below the centre of the Milky Way. These 'Fermi bubbles' extend an astounding 30 thousand lightyears from the plane of the Galaxy.

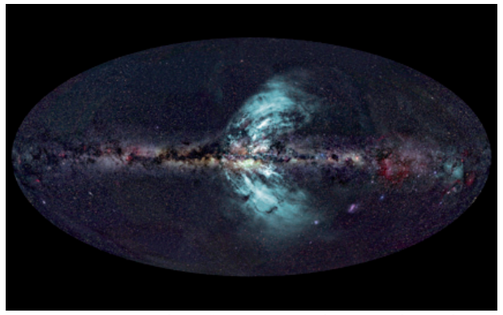

Fig. 14: New-found outflows of particles from the Galactic Centre. The curvature of the outflow is real. [7]

An immediate question posed by the discovery of these Fermi bubbles is: what agent was responsible for their inflation? Was it, in particular, the supermassive black hole that lurks at the centre of the Galaxy or was it, instead, the concentrated star formation occurring around the black hole? In a Letter to PRL in 2011 [6], MPIK researchers presented theoretical arguments supporting the latter viewpoint. The Letter also provided arguments suggesting that the gamma-rays coming from the Fermi bubbles originate in high-energy collisions between cosmic-ray protons and gas rather than from the up-scattering of ambient light by cosmic-ray electrons as had been suggested by others.

In the meantime, follow-up observational work has been performed that seems to support the star-formation picture. Results based on observations by the Parkes radio telescope, published in a Letter to Nature [7], reveal the radio counterparts of the Fermi bubbles (Fig. 14). These counterparts are, in fact, even larger than the Fermi Bubbles, stretching more than half way across the sky. They seem to have been inflated by star formation supporting the original contention made.

Roland Crocker

The Physics of Pulsar Wind Termination Shocks

Pulsar Wind Nebulae (PWNe) are the compact clouds of relativistic, magnetized, electron-positron plasma that surround and are energized by young pulsars – rapidly rotating, strongly magnetized neutron stars. Their non-thermal synchrotron and inverse Compton emission is detected from the radio to TeV gamma-rays – where they make up the majority of the Galactic sources detected by HESS – and it indicates a remarkably flat energy distribution of relativistic particles. Despite decades of research, the mechanism responsible for accelerating these particles in PWNe, which must be drastically different from known astrophysical particle acceleration processes, has remained elusive.

A distinguishing feature of the pulsar winds that inject the energy into PWNe is that they are low-density, magnetized, relativistic plasmas. In such a plasma, strong electromagnetic waves should play an important role. However, these waves are not included in the conventional magnetohydrodynamic description that underlies the theory of particle acceleration at shock fronts in other astrophysical objects. To take them into account requires instead a more elaborate model, for example, one with at least two charged fluids.

In a series of investigations, scientists in the theoretical astrophysics group have studied these waves under pulsar conditions and using a cold two-fluid (electron-positron) description. Stationary, self-consistent solutions describing the interaction of the pulsar wind with the surrounding nebulae were found which suggest the existence of an extended electromagnetic precursor at the termination shock. Such a structure would strongly influence particle acceleration at the shock front, since it controls the ability of particles to cross and recross it, with important observable consequences for the spectra of PWNe. Whilst immensely useful in providing physical insight into this complex problem, the available analytical solutions do not describe the microphysics of wave generation and absorption. To overcome this shortcoming, numerical simulations based on a warm two-fluid model

have been performed. Fig. 15 shows the results. The pulsar wind containing a frozen-in magnetic structure is shown entering the simulation box from the left. The right-hand edge of the box simulates the boundary conditions imposed by PWNe, thus enforcing a termination shock front inside the box. The plasma density is seen to jump sharply at a structure that resembles a shock front in hydrodynamics (top panel). However, strong, counter-propagating electromagnetic waves are generated close to the density jump and build up ahead of it, heating and compressing the incoming wind in an extended precursor. As a result, the incoming energy flux carried by the magnetic field (Poynting flux, lower panel) drops sharply at the upstream edge of the precursor, and remains in rough equipartition with the flux carried by particles into the downstream plasma. This constitutes the first demonstration of an electromagnetically-modified shock front, and is an important advance in the effort to understand the energization of PWNe and the origin of their unusual spectra.

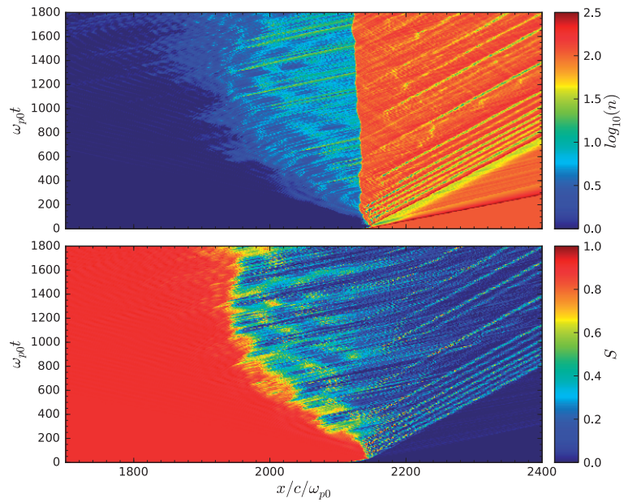

Fig. 15: The plasma density and Poynting flux at a simulated pulsar-wind termination shock (Vertical axis: time, horizontal axis: space) [8].

John Kirk

Radiation of Pulsar Winds

One of the brightest high-energy gamma-ray sources in the sky is the Crab pulsar, from which recently also pulsed very-high-energy radiation has been discovered. In a Letter to Nature[9], MPIK scientists have now presented a compelling explanation for this radiation based on the abrupt acceleration of an ultrafast wind of 'cold' electrons and positrons close to the light cylinder of the pulsar. The generally accepted paradigm postulates the existence of a relativistic pair wind, which originates in the pulsar's magnetosphere and terminates in the interstellar medium where efficient particle acceleration produces an extended non-thermal source: the Crab nebula. While the pulsar has been found to emit high-energy gamma-rays, the radiation of the nebula is released predominantly in the very-high-energy band. The wind, however, despite being the key component via which the transfer of energy from the pulsar to the nebula is realized, has so far evaded observational access. Indeed, despite the extreme relativistic speed of the wind, in the frame of the outflow the electrons are 'cold', meaning that they essentially move together with the wind's magnetic field and therefore do not emit synchrotron radiation. However, as it has turned out now, the wind could reveal itself in high-energy gamma rays through the mechanism of inverse Compton scattering in which ultrafast electrons and positrons of the wind are illuminated by X-ray photons originating in the pulsar's magnetosphere and/or the surface of the neutron star (see Fig. 16). In a Letter to Nature, MPIK researchers argued that recent reports of the surprise detection of pulsed, very-high-energy (VHE) gamma radiation from the Crab are best explained by this process. Accordingly, the detection of the pulsed VHE gamma-ray emission provide the first observational evidence for the formation of a cold ultrafast electron-positron wind from the Crab pulsar. Moreover, the reported gamma-ray data could be used to localize the site and to estimate the speed with which the electromagnetic energy is transformed into the kinetic energy of the wind's bulk motion. A detailed analysis showed that the acceleration of the wind to extreme velocities should take place abruptly in a relatively narrow cylindrical zone of radius between 20 and 50 thousand kilometers centered on the rotation axis of the pulsar. Although the inferred ultrafast nature of the wind does support the general paradigm of pulsar winds, the requirement of the very fast acceleration of the wind in a narrow zone not very far from the pulsar challenges current theoretical models and illustrates the unique potential of gamma-ray astronomy to deepen our understanding of the nature of these objects.

Felix Aharonian

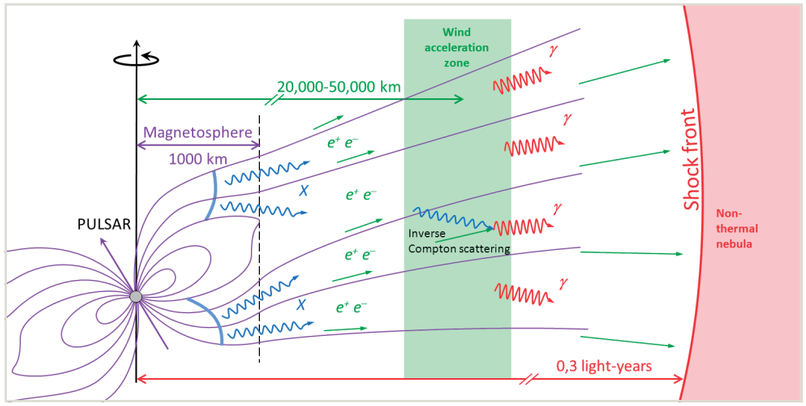

Fig. 16: Schematic evolution of the pulsar wind (electrons and positrons: e^-, e^+). High-energy gamma quanta (γ) are created in the acceleration zone by inverse Compton scattering of the pulsar wind with X-ray quanta (X) from the magnetosphere as well as at large distance at the shock front to the interstellar medium.

Extreme Variability in AGN and the Origin of Relativistic Jets

Active Galactic Nuclei (AGN) are known for their extreme variability behaviour across most of the electromagnetic spectrum. Observations of the extraordinarily bright blazar PKS 2155-304 (distance d ~ 500 Mpc) and the archetypal radio galaxies M87 (d ~ 16 Mpc) with H.E.S.S. during the last couple of years have uncovered that the most rapid variability is apparently occurring in the very-high-energy (> 100 GeV) domain. Causality arguments suggest that this VHE variability should originate in the innermost part of the collimated, relativistic outflows seen from these objects and thus allow a fundamental diagnosis of the inner plasma conditions and nearby source environment.

New results published by MPIK researchers have now shown that this variability could well be caused by the interactions of the jet with ambient gas clouds, as a consequence of which otherwise sub-dominant hadronic emission (pp-collision) processes become significant. This idea, supported by new hydrodynamical simulations, allows one to successfully model the measured VHE spectrum and light curve, inferring important details on the inner magnetic field and energy flux of the jet and on conditions in the ambient medium. In the case of M87, clear evidence for a remarkable interconnection between rapid VHE variability and the ejection of a new radio jet component from the vicinity of its supermassive black hole has been found. Researchers at MPIK have shown that the TeV variability could actually mark the onset of jet formation and thus offer unique insights in the extreme jet processes taking place very close to the black hole. In this picture, strong (gap-type) particle acceleration in the magnetosphere of the black hole and subsequent Compton up-scattering of ambient photons to super-TeV energies triggers a pair cascade that provides the sought-after plasma source for the jet as seen on radio scales. Results like those mentioned above bear the potential to settle a number of unsolved key issues in AGN research and have thus become the backbone of a prominent science case for in-depth exploration with the future CTA instrument.

Frank Rieger, Felix Aharonian

Absorption and the Origin of VHE Emission from Distant AGN

VHE photons from distant AGN have to pass through the Extragalactic Background Light leading to energy-dependent absorption features caused by photon-photon interactions ($\gamma_{VHE}\ \gamma_{EBL} \rightarrow e^+\ e^-$). Interestingly, in the case of some blazars, the gamma-ray spectra after correction for EBL absorption, appear extremely hard with photon indices ≤ 1.5 or even close to 1. This has been considered to seriously challenge conventional radiation models. New results by MPIK researchers show, however, that these findings can be still accommodated within leptonic synchrotron-Compton scenarios, in case time-dependent considerations (e.g. stochastic acceleration and adiabatic losses) are properly taken into account. In fact, the results showed that in external Compton scenarios even harder spectra can be accounted for. Also, the growing number of VHE blazars with redshift exceeding z ~ 0.5 has led to the emergence of theoretical scenarios with far-reaching implications, being based on, e.g., a violation of Lorentz invariance or „exotic" interactions involving hypothetical axion-like particles. Work at MPIK has now shown, however, that even in the framework of standard physics a viable interpretation exists. Provided the intergalactic magnetic field is sufficiently weak ($B \sim 10^{-17}$ - 10^{-15} G) TeV gamma rays can in principle be observed even from a source at z ~ 1, if the observed gamma rays are secondary photons produced in hadronic interactions (with CMB or EBL background photons) of energetic cosmic-ray protons, originating in the blazar jet and propagating over cosmological distances almost rectilinearly. This offers exciting perspectives for further observational research.

Frank Rieger, Felix Aharonian

Infrared Astrophysics: Radiation Fields in Spiral Galaxies

Radiation fields in spiral galaxies arising from direct or dust-reradiated starlight play a central role in heating interstellar gas, and, through their interaction with cosmic-ray electrons, give rise to a major, but hitherto imprecisely constrained component of the high- and very-high-energy gamma-ray emission from these systems. A library of diffuse stellar radiation fields in spiral galaxies was derived using calculations of the transfer of stellar radiation from the main morphological components – disks, thin disks, and bulges – through the dusty interstellar medium. These radiation fields are self-consistent with the solutions for the integrated panchromatic spectral energy distributions (SEDs) previously presented using the same radiation transfer model, incorporating information on the morphology of the galaxies from imaging optical/NIR data, as well as the dust emission SEDs. Because of this, all observables calculated from the radiation fields, such as cooling lines of the interstellar gas or the inverse Compton emission, can be self-consistently predicted from the observationally highly constrained solutions for the ultraviolet/optical/submillimeter SEDs of galaxies. Strongly contrasting solutions are found for the spatial distribution of the radiation fields for disks, thin disks and bulges. For bulges a strong dependence of the radiation fields on Sérsic index is seen. Also, a specific model for the distribution of radiation fields in the Milky Way was produced, to constrain the diffuse inverse Compton emission from the diffuse ISM at GeV energies and predict seed fields giving rise to inverse Compton emission of individual lepton accelerators in the GeV to TeV range. Since dust emission deep in the Rayleigh Jeans regime is an excellent tracer of molecular and neutral gas, this model can also be used to constrain the distribution of targets for the pion-decay component of gamma-ray emission from the diffuse ISM of the Milky Way.

Cristina Popescu, Ruizhi Yang, Richard Tuffs

References:

[1] www.mpi-hd.mpg.de/HESS/pages/10anniversary/;
www.mpi-hd.mpg.de/HESS/pages/home/hess2inaug/;
www.mpi-hd.mpg.de/HESS/pages/press/2012/HESS_II_first_light/
[2] HESS Collaboration, A. Abramowski et al., Astron. Astrophys. 545 (2012) L2.
[3] HESS Collaboration, A. Abramowski et al., Astrophys. Journal 757 (2012) 158.
[4] HESS Collaboration, A. Abramowski et al., Astron. Astrophys. 550 (2013) A4.
[5] HESS Collaboration, A. Abramowski et al., Phys. Rev. Lett. 110 (2013) 041301.
[6] R. M. Crocker and F.Aharonian, Phys. Rev. Lett. 106 (2011) 101102.
[7] E. Carretti, R. M. Crocker et al., Nature 493 (2013) 66.
[8] T. Amano and J. G. Kirk, Astrophys. Journal 770 (2013) 18.
[9] F. A. Aharonian, S. V. Bogovalov and D. Khangulyan, Nature 482 (2012) 507.

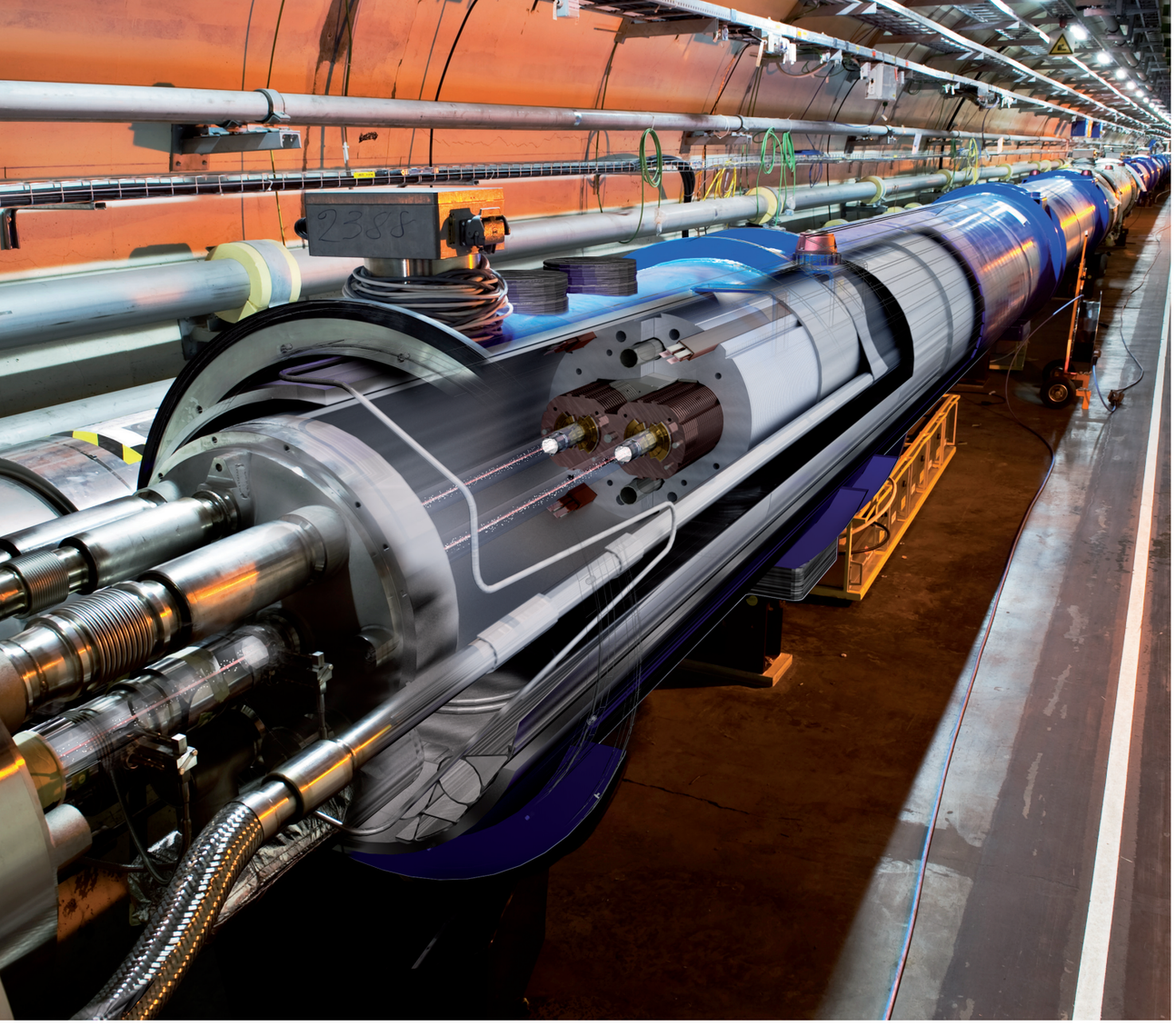

1.2 Particle Physics at Accelerators

Tunnel of the Large Hadron Collider (LHC) at CERN. The cut-away view of one of the superconducting magnets shows the two beam pipes for the counter-circulating beams, which can be steered into collision in four interaction regions. (Image: CERN)

Introduction

Currently the energy frontier for accelerator based particle physics is set by the Large Hadron Collider (LHC) at CERN, Geneva. The ring has a circumference of 27 km, is located at a depth of about 100 m under ground and allows to accelerate and to collide protons and lead nuclei. It's physics mission is to study the Higgs particle which in the Standard Model determines the masses of the fundamental particles, to search for New Physics beyond the Standard Model and to study nuclear matter under extreme conditions by means of heavy ion collisions. In its first running period between the end of 2009 and February 2013 the LHC reached nucleon-nucleon center-of-mass energies of 8 TeV for proton-proton collision, 5 TeV for proton-lead collisions and 2.76 TeV for lead-lead collisions.

The four large experiments at the LHC were optimized for Higgs physics and the search for new heavy particles (ATLAS and CMS), for the study of heavy ion-collisions and the quark-gluon plasma which can be produced in such interactions (ALICE), and for precision measurements of CP-violation and rare decays in the heavy flavor sector (LHCb).

At LHCb particles containing b-quarks are produced with rates on the order of 100 kHz, with the consequence that already three years after the start of the LHC the experiment begins to dominate the field of flavor physics. Many measurements probe quantum corrections to the Standard Model and thus are susceptible to effects from new virtual particles, thereby looking for New Physics in a way complementary to, but with similar sensitivity as the direct searches for new particles by the general purpose detectors ATLAS and CMS. In addition, LHCb with its excellent tracking, vertexing and particle identifications capabilities in a kinematical region not accessible to the other experiments is also making essential contributions to electroweak and QCD studies.

A schematic view of the LHCb detector is shown in Fig. 1. It has been designed to record the complete information of all particles emitted in inelastic collisions into the angular range between 15 and 300 mrad with respect to the beam. Charged particles produced at the collision point are recorded by means of a magnetic spectrometer, photons and neutral particles are detected using calorimeters. Cherenkov detectors and muon system serve to identify the particles, and an elaborate filter system selects those events from the sample of all the interactions which contain information about the physics questions investigated with LHCb. Up to 5000 potentially interesting events per second can be stored for further analysis. In 2012, more than 20 billion events and a data volume of more than 1 petabyte has been recorded. The analysis of the data is done within the world-wide LHC computing grid.

The experiment is operated by an international collaboration of scientists from 64 institutes in 16 countries. The LHCb detector has about a million read-out channels, nearly half of which are equipped with silicon sensors. The MPIK has contributed the "Beetle" front-end chips for all of these components, the complete read-out electronics for

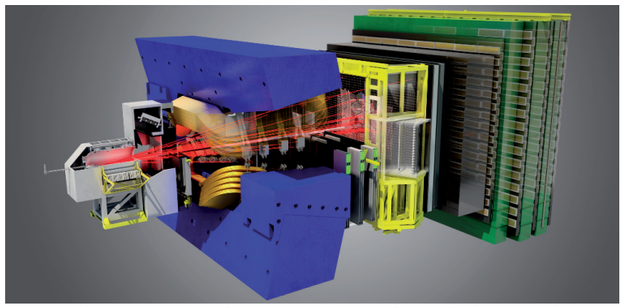

Fig. 1: Schematic view of the ca. 20 m long and 10 m high LHCb detector. The collision point is to the left of the spectrometer magnet (blue). Parts of the tracking system and the Cherenkov detectors are visible on both sides, to the right follow calorimeter and muon system.

half of them, and a sizable fraction of the sensors. The chips are an in-house development because commercially available devices would not withstand the radiation environment of the experiment. In the following a few physics highlights will be presented where the MPIK had a significant share in the results obtained by the LHCb experiment.

Forward Energy Flow

The final state of inelastic proton-proton interactions is the result of hard and soft scattering processes between the constituents of the collision partners. While the hard component can be described by perturbative QCD, the soft component is much less amenable to a theoretical treatment and progress in this field still requires experimental input.

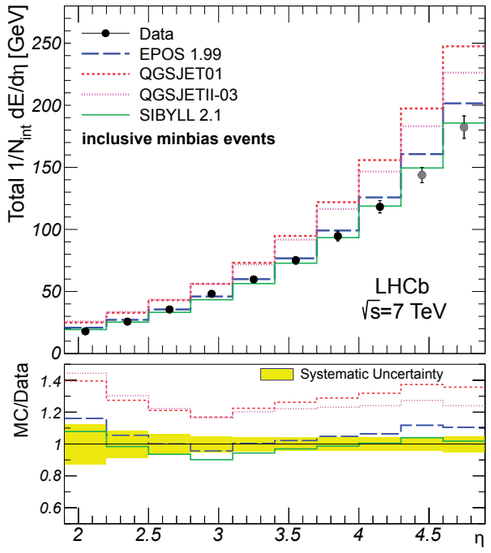

Fig. 2: Forward energy flow measured by the LHCb experiment compared to predictions from cosmic ray interaction models.

A fundamental observable is the total energy emitted into a certain angular interval per inelastic proton-proton collision. This so-called "energy flow" integrates over all processes contributing to final state particle production, and has been measured by the LHCb experiment [1] for different event classes at forward angles in the range between 15 and 300 mrad with respect to the beam direction, corresponding to pseudo-rapidities $1.9<\eta<4.9$.

Fig. 2 shows the energy flow for inelastic proton-proton interactions selected with the loose requirement of having seen at least one charged particle track inside the detector ("inclusive minimum bias events"). The points are the experimental measurements, the histograms show predictions by models which are used in cosmic ray physics to describe the interaction of high energy cosmic ray primaries with the earth's atmosphere. Given the fact that these models were developed to describe observables in cosmic-ray physics, e. g. particle densities at ground level created in extensive air showers, the agreement is surprisingly good. It is of the same or better quality as models used in particle physics (not shown) which were adjusted to data recorded prior to the LHC. Interestingly, while cosmic-ray interaction models tend to overestimate the energy flow, it is underestimated by the particle physics models.

Prompt Charm Production

Protons consist mainly of up-quarks (u), down-quarks (d) and gluons. Heavier quarks contribute only through vacuum fluctuations where the still relatively light strange quarks (s) are most prominent. From the heavy flavors only charm-quarks (c) provide a visible but small contribution, the share of bottom (b) and top-quarks (t) is negligible.

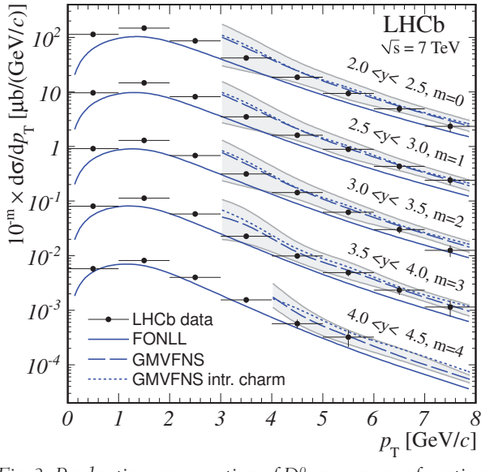

Fig. 3: Production cross-section of D^0-mesons as a function of transverse momentum for rapidity bins in the range $2.0<y<4.5$.

The production of particles containing charm quarks in high energy proton-proton interactions therefore requires those quarks to be produced in the collision. Since charm quarks are already sufficiently heavy to provide a hard scale, the production process can be described by perturbative Quantum Chromodynamics (QCD). Charmed hadrons then can be produced either directly or via feed-down from decays of very short-lived excited charm resonances. Both are commonly referred to as "prompt", featuring an initial hard process, the production of a $c\bar{c}$-pair, for which theoretical predictions exist. Alternatively, charmed hadrons are also produced in decays of longer lived b-hadrons, where the lifetime of the mother particle allows to separate this background contribution from the prompt component.

The LHCb experiment has measured the production cross-section of prompt $D^0(c\bar{u})$, $D^+(c\bar{d})$, $D_s^+(c\bar{s})$ and $D^{*+}(c\bar{b})$ mesons and of the $\Lambda_c^+(udc)$ baryon [2]. The quark content of each particle type is given in parentheses. The measurement was performed in proton-proton collisions with a center-of-mass energy of 7 TeV for transverse momenta of the charmed hadrons $0<p_T<8$ GeV/c and rapidities $2.0<y<4.5$ in the proton-proton center-of-mass system. This kinematic region that has not been accessible in the past and cannot be studied by the other LHC experiments either.

Fig. 3 shows a comparison between the measured differential cross-section for the production of D^0-mesons and current theoretical predictions, plotted as a function of transverse momentum for different rapidities. Since the rapidity dependence is weak, for better visibility the cross-sections measured in subsequent rapidity intervals are scaled by factors of 10. The points represent the LHCb measurements, the lines are theoretical predictions for different models which differ by up to a factor of two in the cross-section, but still agree within the theoretical uncertainties indicated by the grey bands. Within the rather large uncertainties of the predictions good agreement between data and theory is observed. One also sees that for the kinematic region of this measurement the contribution from intrinsic charm in the proton is negligible.

Cold Nuclear Matter Effects in Proton-Lead Collisions

A quark-gluon plasma can be characterized as an extremely hot and dense gas of free quarks and gluons which existed in the early universe before the primordial nucleosynthesis, and is expected to be created also in ultra-relativistic heavy ion collisions. One of the predicted signatures for the existence of a quark-gluon plasma is the suppression of the production of J/ψ mesons (bound charm-anticharm states) with respect to the production observed in proton-proton collisions. However, such a suppression can also occur due to cold nuclear matter effects through modifications of the parton densities of nucleons bound inside a heavy nucleus, or as a consequence of energy loss of the produced charm quarks in the nuclear environment.

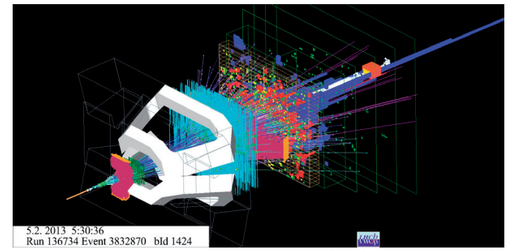

Fig. 4: Visualisation of a proton-lead collision at LHCb. The high density of particle tracks emerging from the interaction point is clearly visible.

The effect of cold nuclear matter can be studied in proton-lead collisions, where a quark-gluon plasma cannot be formed. In February 2013 LHCb participated in the proton-lead run of the LHC in order to address this issue. Fig. 4 gives an impression of the large number of tracks created in a typical proton-lead collision, which on average is between two and three times larger than in proton-proton collisions of the same center-of-mass energy.

Experimentally J/ψ mesons are reconstructed from their decay into muon pairs which are identified by the muon system of the detector. Because of its excellent vertexing capabilities LHCb can also distinguish between prompt J/ψ production, for which theoretical predictions exist, and J/ψ mesons from b-decays. The effect of the nuclear environment can be quantified by the so-called nuclear suppression factor R_{pPb}, defined as the ratio between the production cross-section per collision partner in proton-lead and proton-proton collisions. Fig. 5 shows the result as a function of the rapidity of the J/ψ meson [3], compared to various theoretical predictions. In the forward hemisphere $y>0$, where the produced J/ψ meson has to traverse more nuclear matter than in the backward direction, a clear suppression is observed. The measurements are in agreement with the theoretical predictions, which still suffer from large uncertainties as indicated by the shaded bands. The results suggest that both modifications to the parton densities in the target nucleons and energy loss play a significant role in these processes. Doing the same studies with heavier particles will allow to disentangle the two contributions.

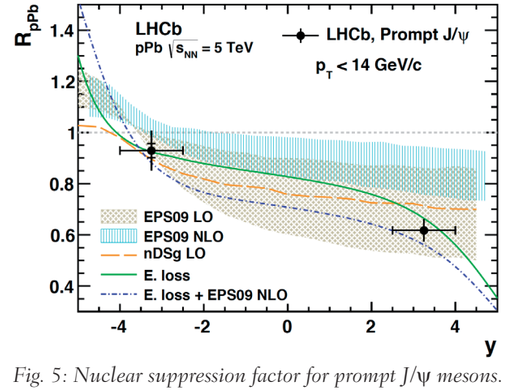

Fig. 5: Nuclear suppression factor for prompt J/ψ mesons.

Michael Schmelling

References:

[1] LHCb Collaboration, Eur. Phys. J. C73 (2013) 2421.
[2] LHCb Collaboration, Nucl. Phys. B 871 (2013) 1-20.
[3] LHCb Collaboration, arXiv:1308.6729.

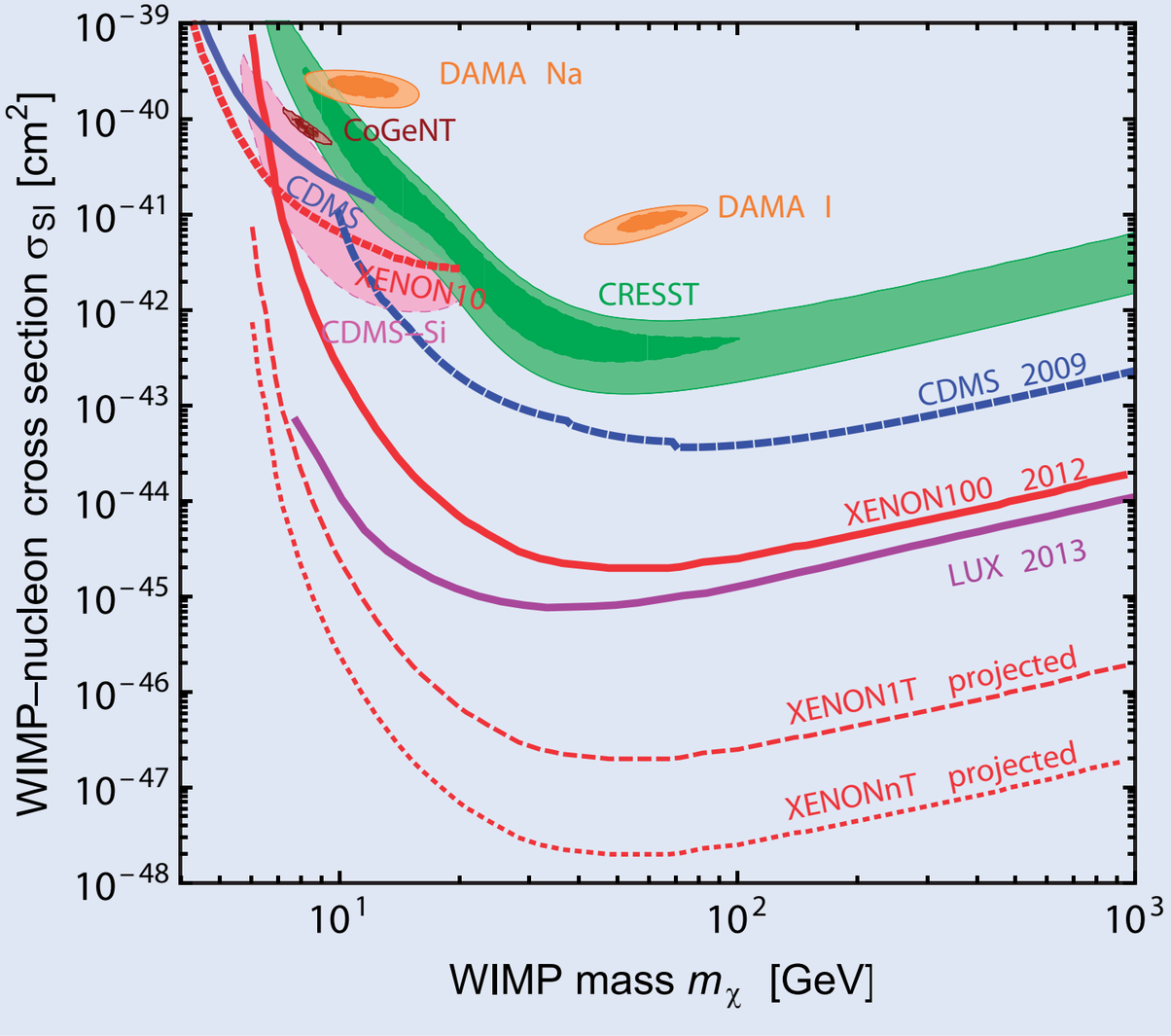

1.3 Dark Matter

The allowed regions and exclusion limits from various Dark Matter experiments in the plane of Dark Matter mass and spin-independent scattering cross section.

Introduction

One of the biggest open questions in today's particle physics and cosmology is the identification of the Dark Matter in the Universe. A large collection of cosmological as well as astrophysical observations show strong evidence that a large fraction of the matter in the Universe (Fig. 1) cannot be made out of the known forms of matter, consisting of protons, neutrons, and electrons. Extensions of the Standard Model of particle physics, which are anyway required for other reasons, contain often so-called Weakly Interacting Massive Particles (WIMPs) which are ideal Dark Matter (DM) candidates. Their properties imply that the right magnitude of Dark Matter was automatically produced in the Big Bang and they also fit to all other indirect astronomical and cosmological evidences.

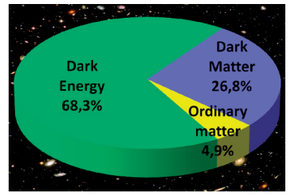

Fig. 1: The composition of the Universe.

The XENON Dark Matter Experiments XENON100, XENON1T and XENONnT: Probing the WIMP Hypothesis with Unprecedented Sensitivity

In recent years deep underground experiments have made a breakthrough in sensitivity towards directly testing the WIMP hypothesis. From the very beginning of operation at the Gran Sasso underground laboratory (LNGS) in late 2009 the XENON100 experiment [1] has been playing a leading role in the search for direct evidence of Dark Matter interaction with ordinary nuclei. Since then, the group at MPIK has made essential contributions to the successful detector operation and analysis of collected data.

The core of the experimental setup is a dual-phase liquid xenon time projection chamber (TPC) acting as a target to observe the scattering of WIMPs. Two arrays of 242 one-inch photo-electron multiplier tubes (PMT) in total are mounted on top and at the bottom of the cylindrical TPC to watch out for even tiny light signals. Applying the detection of both, signals from scintillation photons (S1) and signals generated by ionization electrons in the gaseous xenon phase (S2), enables to reconstruct the spatial interaction vertex in all three dimensions and to discriminate between common radiation background and expected WIMP signals. The whole inner detector is contained in a cryogenic vessel and both are enclosed by a passive radiation shield to protect the setup from environmental radioactivity and from neutron penetration.

Two major science runs have been performed and reported until the time of writing. They cover analyses of 110 and 225 live days of data taken at unprecedentedly low background conditions [2]. Due to the application of only radio-pure construction materials, powerful self-shielding of the liquid xenon and efficient rejection of multiple scattering events one has achieved a background rate index in the dark matter relevant search range of just a few 10^{-3} events/kg/day/keV. In parallel, the collaboration has introduced and established the concept of the „profile likelihood" analysis in the context of direct dark matter searches. It naturally allows taking into account the distribution of known backgrounds and the expected signal shape in order to provide a more accurate testing of the dark matter interaction hypothesis on a given data set.

The observation of only two event candidates in the 225 live-days analysis – essentially consistent with statistical fluctuation of the expected background – has consequently allowed to derive the most sensitive exclusion limit at that time on the elastic, spin-indepen-

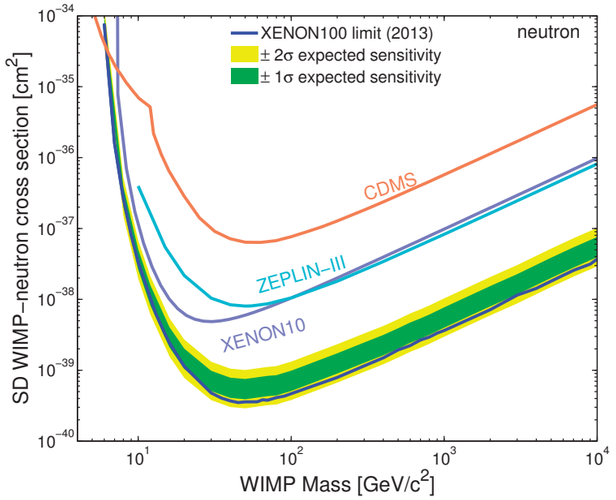

Fig. 2: XENON100 exclusion limits on the WIMP spin-dependent scattering on neutrons compared to previous limits from XENON10, CDMS, ZEPLIN-III. For details see [3].

dent WIMP-nucleon interaction, with a minimum cross-section of 2×10^{-45} cm^2 at 55 GeV/c^2 WIMP mass (see Fig. 2). The null finding of XENON100 has recently been confirmed by the LUX experiment employing the identical detection principle. At the same time other interactions models, e.g. the spin-dependent coupling of WIMPs to ordinary nuclei, could be probed and thus, existing bounds further constrained. State-of-the-art nuclear shell models were accounted for in the related publication to surpass existing standards related to the underlying theoretical calculations [3].

Another benchmark was the detailed analysis of the nuclear recoil detector response based on data taken by calibration with an AmBe neutron source [4]. The neutral WIMP is supposed to cause the same signal signature defined by the transfer of recoil energy directly to the nucleus instead of atomic shell electrons. Comparing the calibration data with results from a dedicated simulation of the full interaction processes, it became possible to extract defining properties of scintillation and charge ionization in LXe due to nuclear scattering. These findings did not only confirm the applied energy scale (currently derived from the S1 signal) but will also become essential to enhance the energy information by using the S2 channel in the near future. This analysis, the evaluation of science run data and many other important studies adding to the understanding of background have been carried out with significant contributions by the MPIK group.

The next step in the successful series of XENON experiments is XENON1T. Based on the same technique as XENON100 it employs about 3 tons of active xenon target mass and will boost the sensitivity for the WIMP-nucleon cross section by two orders of magnitude. Its TPC will be equipped with two arrays of 121 and 127 three-inch PMTs, respectively, watching out for signals in the liquid xenon target from above and below. The liquid xenon target and the TPC are enclosed in a stainless-steel cryostat that will be immersed in the center of a 9.6 m diameter water tank (Fig. 3). The ultra-pure water acts as a passive shield and simultaneously as an active Cherenkov veto detector against residual cosmic muons at the underground site of the experiment in hall B at Laboratori Nazionali del Gran Sasso (LNGS) in Italy. XENON1T is fully funded and the construction phase of the experiment started in summer 2013. Construction will continue during 2014 and the commissioning phase is expected to begin early 2015. XENON1T is designed to probe the bulk parameter space predicted by supersymmetric extensions of the standard model of particle physics. Thus, after a few years of running, XENON1T will either discover the long-sought WIMP or disfavor the WIMP hypothesis as explanation for the dark matter puzzle. The XENON1T experiment allows for a fast upgrade called XENONnT. About 6 tons of liquid xenon will be employed therein while most hardware items of XENON1T like cryostat and cryogenic systems, water tank, infrastructure building, xenon storage vessel as well as gas handling system will be re-used.

Fig. 3: Water tank for XENON1T installed in hall B of LNGS.

A big challenge for XENON1T is the suppression of radioactive backgrounds in the fiducial volume of the detector to an unprecedented low level. This holds for both, external background induced by gamma-ray emitting isotopes in the detector construction materials and internal background caused by disintegrations of radioactive nuclides that are dissolved in the liquid xenon target. The latter one cannot be suppressed by self-shielding and scales with the mass of the xenon target. The most critical contaminants of this kind are ^{85}Kr and ^{222}Rn. Natural krypton is present in commercially available xenon at the ppb level as a by-product of the xenon production process. It contains the radionuclide ^{85}Kr which is mainly produced in nuclear fuel reprocessing plants. To achieve the challenging background goal of about 0.05 events/kg/day/keV in the energy range relevant for the Dark Matter search, a Kr/Xe concentration of about 0.5 ppt is necessary. This will be achieved by performing on-site xenon distillation with a dedicated cryogenic distillation column developed by the XENON1T collaboration. However, the validation of such low krypton levels requires the detection of krypton in xenon at sub-ppt level which is a completely non-trivial task. The

XENON collaboration has been successfully following complementary strategies to approach this issue: in-situ measurement of the ^{85}Kr concentration inside the XENON100 detector using the delayed-coincidence method, measurements employing atomic trap trace analysis (ATTA) and a rare-gas mass spectrometery (RGMS) assay. The latter one was developed and is performed at MPIK. This technique combines a gas chromatographic procedure to separate efficiently the krypton fraction from the bulk xenon gas and a highly sensitive krypton detection by a sector field mass spectrometer. After a thorough calibration the system was shown to achieve a detection limit of 8 ppq [5] surpassing existing techniques by about two orders of magnitude. This is sufficient not only for the XENON1T experiment but also for its upgrade XENONnT. Fig. 4 shows a summary of results obtained with this device.

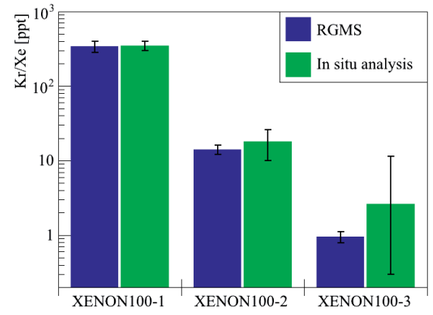

Fig. 4: The measured Kr/Xe ratio during three science runs of XENON100. The off-line RGMS assay is in excellent agreement with the in situ analysis, however, the RGMS technique is more sensitive to low krypton concentrations.

The other challenging internal contamination of xenon is ^{222}Rn. It is relatively short-lived (half-life of 3.82 days), so an initial ^{222}Rn contamination decays away quickly. However, ^{222}Rn is produced in the primordial ^{238}U decay chain and trace impurities of uranium are present in basically all construction materials. Thus, ^{222}Rn is permanently produced internally and may be transported to any place inside the detector.

In the XENON100 experiment the collaboration has developed a solid understanding of the radon and its subsequent decay processes by analyzing in data both alpha decay and delayed-coincidence signatures within the detector [4]. Simulations show that the intrinsic ^{222}Rn concentration in LXe should not exceed the level of 1 µBq/kg. Fulfilling this requirement means another factor 50 reduction of the intrinsic radon contamination in LXe with respect to the current achievements. One possible way of reducing the amount of radon is provided by careful material selection prior to the actual building phase. Here, gamma ray screening for ^{226}Ra is often not sufficient. MPIK employs miniaturized proportional detectors to count alpha disintegrations subsequent to the ^{222}Rn decays. These devices, originally developed at MPIK for application in the GALLEX/GNO solar neutrino experiments feature a very low background for alpha particle detection of about 1 count per day. Three gas handling and counter filling lines and dedicated procedures to extract radon from basically any sample and to load it to the proportional counter were developed during the last years (see previous MPIK progress reports). It is possible to detect as few as 10 emanated ^{222}Rn atoms with this technique, which corresponds to a sensitivity of about 20 µBq. Such low detection limit is necessary to discover and eliminate radon in XENON1T, because usually tiny radon emanation from many sources adds up to a non-negligible amount.

To reduce ^{222}Rn to even lower levels XENON1T is foreseen to be equipped with a radon removal system, aiming at the constant purification of the LXe target from emanated radon during detector operation. The principle idea is separating the radon from the xenon by retaining the radon outside the active detector volume until it naturally disintegrates via radioactive decay. The currently investigated separation techniques are based either on adsorption or cryogenic distillation. If an adsorption system is chosen, its performance strongly depends on the properties of the selected adsorbent. Therefore, at MPIK a dedicated facility has been developed to probe different materials on their capability to adsorb radon within a xenon environment but also in terms of mechanical stability and radio-purity. Cryogenic distillation is a challenging, but very attractive alternative. Recently, a R&D program at MPIK has started which studies possible technical designs of such a radon distillation plant.

MPIK is also responsible for testing the photo sensors in XENON1T. They are required to have a very low intrinsic radioactivity, high quantum efficiency at the LXe scintillation wavelength of 175 nm, to operate stable at –100 °C and to have a good single photon resolution. To guarantee that the R11410-21 PMT developed by Hamamatsu for XENON1T fulfills all these needs, a series of test are performed at LNGS and at MPIK in Heidelberg. Upon delivery each batch of PMTs is sent for screening to LNGS where low background germanium spectrometers determine their internal radioactive contamination. Afterwards the PMTs are transported to MPIK where the PMTs are mounted into a testing facility developed originally for Double Chooz (see progress report 2007-2008). This setup is inside a Faraday dark room where 12 PMTs can be tested simultaneously with low noise conditions. Blue LEDs are installed in front of each PMT such that the intensity can be adjusted individually. Dark count rate, gain at different voltages, after pulsing probability and timing

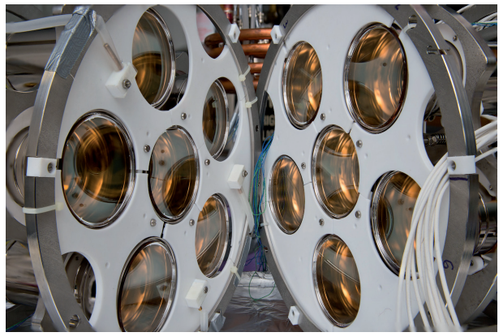

Fig. 5: Support structures for cooling tests of XENON1T PMTs at MPIK.

properties are measured in order to characterize the basic PMT performance.

In order to test the robustness of the PMTs after cooling down/warming up, a new setup has been built. It consists of a vacuum-insulated tank which is filled with nitrogen vapor and cooled down using liquid nitrogen flowing through a copper coil. Two structures with 6 PMTs each are installed inside, (see Fig. 5). Each PMT is cooled down three times and its properties at cold temperatures are recorded. The first 60 PMTs have been already tested. Similarly, the remainder of the PMT production will be characterized. The installation of the tubes in the support structure for XENON1T is planned for middle 2014.

Manfred Lindner, Teresa Marrodán Undagoitia, Hardy Simgen

Dark Matter Phenomenology

Weakly Interacting Massive Particles, i.e., stable particles with properties typical for the scale of weak interactions of around 100 GeV, are very well motivated Dark Matter candidates. The Standard Model of particle physics suffers from a conceptual problem, the so-called hierarchy problem. Roughly speaking it means that if there is new physics at an energy scale larger than the weak scale, the theory has to be exceedingly fine-tuned in order to cancel divergent quantum contributions and keep the mass of the Higgs boson at the observed value of 126 GeV. In order to avoid this problem, theorists are expecting new physics to appear not too far away from the weak scale. One of the most interesting options for this new physics is Supersymmetry (SUSY), which offers a particularly attractive way to avoid the divergent quantum effects. Interestingly, often theories addressing the hierarchy problem predict also a stable particle serving potentially as DM candidate, for instance in SUSY the so-called neutralino. Furthermore, for a stable particle with interactions typical for the weak scale a simple physical process in the early Universe called „thermal freeze-out" leads approximately to the correct abundance in order to provide the Dark Matter. Hence, the link of new physics close to the weak scale motivated by the hierarchy problem with the thermal freeze-out mechanism makes WIMPs an attractive DM candidate.

The attractive feature of WIMP DM is that the requirement of a successful freeze-out mechanism in order to obtain the correct DM abundance allows to predict within a certain range the scattering cross section searched for in direct detection experiments. This idea has been investigated in [6] in the context of the minimal supersymmetric extension of the Standard Model (MSSM). Fig. 6 shows the predicted range of the scattering cross section compared to current experimental limits and future sensitivities. The color-coding in the plot indicates the internal fine-tuning of the theory. It follows that for natural theories with little fine-tuning (green points) relatively large cross sections are predicted, partially already excluded by current data. Small cross sections require exceedingly strong tuning in the theory (red points), which contradicts one of the main motiviations of the MSSM, namely addressing the fine-tuning related to the hierarchy problem. The results of [6] suggest that the WIMP hypothesis in the context of „natural" versions of the MSSM will be tested by direct detection experiments in the near future.

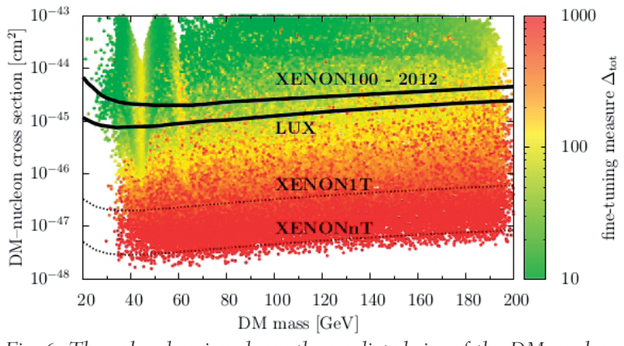

Fig. 6: The colored region shows the predicted size of the DM-nucleus scattering cross section for thermally produced supersymmetric DM with the correct abundance in the Universe. The color coding shows the internal fine-tuning of the theory, where the scale on the right indicates the amount of fine tuning: e.g., red corresponds to tuning within 1 in 1000. Also shown are the current limits from the XENON100 and LUX experiments (solid curves), as well as future expected sensitivities (dotted curves). Figure adapted from [6].

Apart from the above mentioned limits on the DM-nucleus scattering cross section there are also several experiments reporting results which may be interpreted in terms of a positive DM signal. The DAMA/LIBRA experiment finds strong evidence for an annualy modulated event rate, in agreement with the expectation from the DM signal, induced by the rotation of the Earth around the Sun. The CoGeNT, CRESST-II, and CDMS-Si experiments find excess events above their expected background. All those results may be interpreted in terms of a DM particle with mass around 10 GeV. However, the required cross sections are in tension with bounds from XENON100, LUX, and other experiments. The regions in the plane of DM mass and spin-independent scattering cross sections, which can explain the above mentioned hints for a positive signal as well as bounds from various experiments are shown in the title picture.

Various types of phenomenological studies have been performed in order to investigate possible ways to reconcile the hints among themselves and with the limits by considering variations in the particle physics governing the type of DM-nucleus interaction as well as considering uncertainties in the local velocity distribution of DM particles. For instance, in [7] the problem of astrophysical uncertainties has been studied by adopting a self-consistent model for the Milky Way, motivated by N-body simulations and fitted to actual observational data. In particular the impact of anisotropy in the DM velocity distribution has been investigated. It has been found that those effects cannot improve the consistency of the data. In [8], a method has been developed to compare a possible annual modulation signal (such as seen in the DAMA/LIBRA experiment) to limits from other experiments, such as XENON100, largely independent of astrophysics. It has been shown that limits from XENON100 exclude a DM interpretation of DAMA/LIBRA at very high confidence level, based only on very weak assumptions about the properties of the DM halo, for a number of different particle physics models for the DM-nucleus scattering cross section.

Another way to search for WIMP DM is through the observation of characteristic spectral features in cosmic rays due to the self-annihilation of DM particles in regions of high DM concentration, such as the galactic center. Ref. [9] has considered the implications for DM properties of the recent measurement of the fraction of positrons to electrons in cosmic rays by the AMS-02 experiment at the international space station. It has been shown that due to the yet unexplained positron excess, limits on DM properties are generally weaker than those obtained using other probes, especially gamma rays. This also means that explaining the positron excess in terms of dark matter annihilation is difficult. Only if very conservative assumptions on the dark matter distribution in the galactic center region are adopted, it may be possible to accommodate dark matter annihilating to leptons with a cross section large enough to explain the positron excess. Connections between gamma-ray spectral lines in cosmic rays from DM annihilations and signatures at the LHC at CERN and other connections between DM and other experiments have been studied in further publications.

Finally we mention also research on non-WIMP DM candidates, which may become more and more attractive if currently ongoing WIMP searches do not find a convincing positive signal. In particular, sterile neutrinos with masses in the few keV range provide an alternative candidate for DM, in general not related to physics at the weak scale. Such particles are produced in a non-thermal way in the early Universe and are called warm DM. They might lead to a slightly different history of structure formation than in the standard cold DM scenario, predicting less structure at small (sub-galaxy) scales. Various aspects of keV sterile neutrino DM have been investigated in different publications, see e.g. [10].

Joachim Kopp, Manfred Lindner, Thomas Schwetz-Mangold

References:

[1] E. Aprile et al. [XENON100 collaboration], Astropart. Phys. 35 (2012) 573-590.
[2] E. Aprile et al. [XENON100 collaboration], Phys. Rev. Lett. 105 (2010) 131302 and Phys. Rev. Lett. 107 (2011) 131302 and Phys. Rev. Lett. 109 (2012) 181301.
[3] E. Aprile et al. [XENON100 collaboration], Phys. Rev. Lett. 111 (2013) 021301.
[4] M. Weber, PhD Thesis, University of Heidelberg (2013).
[5] S. Lindemann and H. Simgen, arXiv:1308.4806.
[6] P. Grothaus, M. Lindner and Y. Takanishi, JHEP 1307 (2013) 094.
[7] N. Bozorgnia, R. Catena and T. Schwetz, arXiv:1310.0468.
[8] J. Herrero-Garcia, T. Schwetz and J. Zupan, Phys. Rev. Lett. 109 (2012) 141301.
[9] J. Kopp, Phys. Rev. D88 (2013) 076013.
[10] F. Bezrukov, A. Kartavtsev and M. Lindner, J. Phys. G40 (2013) 095202.

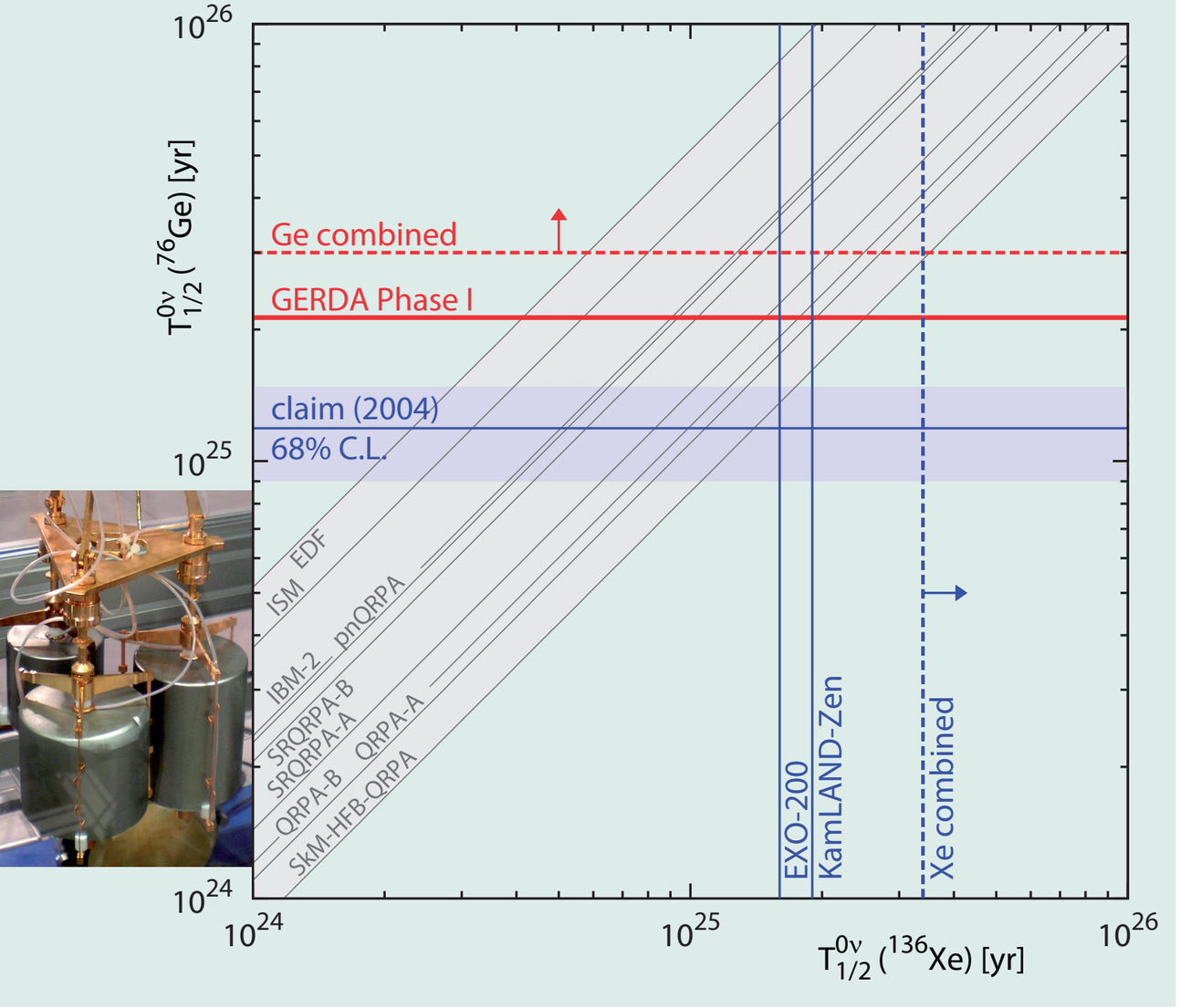

1.4 Neutrinos

Comparison of the best lifetime limits for neutrinoless double beta decay from experiments using ^{136}Xe (vertical lines) and ^{76}Ge (horizontal lines, including the previous claim of the Heidelberg-Moscow experiment). The diagonal lines show calculations which relate the two measurements. Due to theoretical uncertainties, these cover a wide range illustrating why Ge-based experiments are best suited to scrutinize the previous claims [3].

Introduction

While the Standard Model of particle physics (SM) is a very successful theory, there are very strong theoretical arguments that at higher energies it must be embedded into a new theory. Currently, there is however only one solid evidence for new physics beyond the Standard Model: massive neutrinos. The SM assumes them to be massless particles, but neutrino oscillation experiments have shown without doubt that neutrinos possess non-vanishing rest masses. It is therefore of crucial importance to study neutrinos both experimentally and theoretically in order to understand their nature and the origin of their masses, mixings, CP phases and symmetry properties.

The Search for Lepton Number Violating Neutrinoless Double Beta Decay with the Germanium Detector Array (GERDA)

The Germanium Detector Array (GERDA) experiment was built for the search of the neutrinoless double beta decay ($0\nu\beta\beta$) in ^{76}Ge according to $^{76}\mathrm{Ge} \rightarrow {}^{76}\mathrm{Se} + 2e^-$ [1]. The observation of that decay, a peak at the Q-value $Q_{\beta\beta}$ of this process, would prove that lepton number is not conserved, and that neutrinos and antineutrinos have the same identity. A discovery would have significant implications on particle physics and other fields, including cosmology. The first phase of the GERDA experiment started in November 2011, and has since yielded the best limit for the half life $T^{0\nu}_{1/2}$ of the $0\nu\beta\beta$ decay and refuted the claimed observation of the $0\nu\beta\beta$-decay by a subgroup of the Heidelberg-Moscow experiment. A second phase of GERDA is currently under preparation.

GERDA is operated underground in the Laboratori Nazionali del Gran Sasso covered by an overburden of 1400m of rock. The main feature of the GERDA design is the operation of bare germanium detectors in liquid argon (see Fig. 1). The detectors are isotopically enriched in ^{76}Ge. Liquid argon serves both as a cooling medium for the detectors, and as a high purity shield against background radiation. The detector supports and front end electronics are designed for minimal mass and meet stringent radiopurity requirements. The argon cryostat is placed in a water tank which acts as a passive shield against external radiation from the experimental hall, such as neutrons, as well as an active Cherenkov muon veto system.

Progress of GERDA: construction, commissioning: GERDA Phase I became fully functional in summer 2010. First commissioning runs with natural germanium detectors revealed that background from ^{42}K (daughter of cosmogenic ^{42}Ar) is at least ten times higher than was predicted from literature values used in the GERDA proposal. Henceforth, this background was

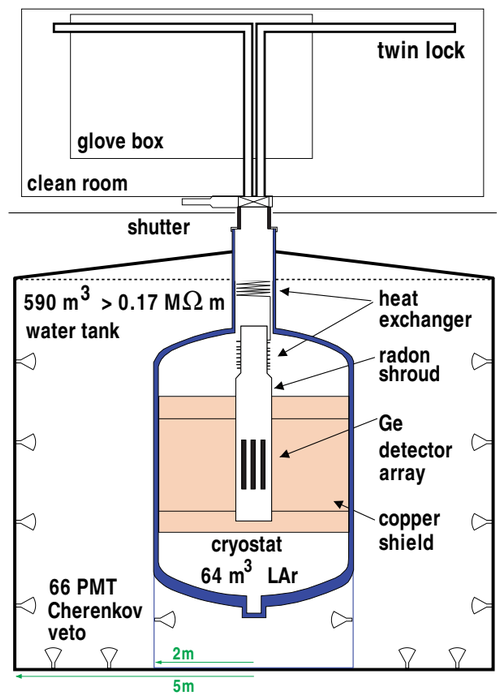

Fig. 1: Schematic drawing of the main components of the GERDA experiment.

investigated thoroughly in GERDA and the LArGe test facility. A dedicated campaign in LArGe with liquid argon spiked with additional ^{42}Ar was carried out to study the collection process of ^{42}K ions in the presence of electric fields: it was found that copper ‚mini-shrouds' around the detectors sufficiently suppress the ^{42}K background below the required level of Phase I. Subsequently, all eight enriched HPGe coaxial detectors were deployed, as well as three HPGe detectors from natural germanium, and five new enriched detectors of Broad Energy Germanium (BEGe) type with superior pulse shape discrimination properties. In November 2011 the commissioning was concluded and the phase I physics run started.

Phase I results: After 126 life days of data taking the GERDA data was analysed for the half life of the two neutrino double beta ($2\nu\beta\beta$) decay: it yielded an improved value of $T^{2\nu}_{1/2} = (1.84^{+0.14}_{-0.10}) \times 10^{21}$ yr. Such a precision with moderate statistics is only possible due to a much lower background level of GERDA compared to predecessor experiments.

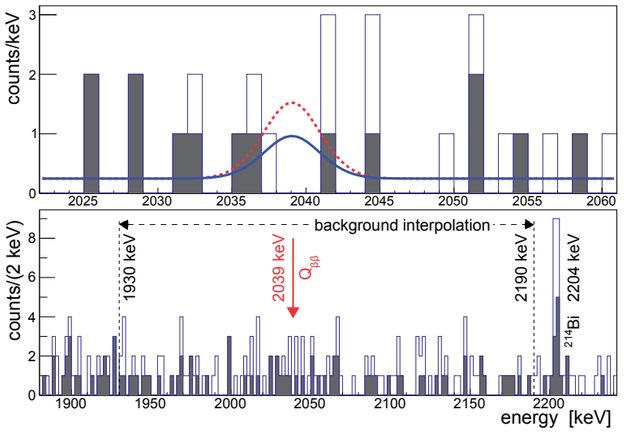

Fig. 2: The combined energy spectrum from all enriched Ge detectors without (with) PSD is shown by the open (filled) histogram. The lower panel shows the region used for the background interpolation. Curves in the upper panel show the expectations (for the PSD selection) based on the central value of the claim, $T^{0\nu}_{1/2} = 1.19 \times 10^{25}$ yr (red dashed), and with the 90% upper limit derived in this work, corresponding to $T^{0\nu}_{1/2} = 2.1 \times 10^{25}$ yr (blue solid).

The Phase I physics analysis of of the neutrinoless double beta ($0\nu\beta\beta$) decay uses data collected until May 2013 (492.3 live days). The total exposure amounts to 21.6 kg·yr. In order to avoid human bias the data was blinded in a 40 keV energy window around the expected peak position of the $0\nu\beta\beta$-decay. Prior to unblinding this region the collaboration decided upon the employed automated analysis procedure and fixed all relevant cut parameters, including those for the desciption of the background and pulse shape discrimination (PSD). The background model and treatment in the subsequent analysis as well as the various methods used for PSD were documented and published in a dedicated paper [3]. The achieved background index after PSD is $(11 \pm 2) \times 10^{-3}$ cts/(keV·kg·yr) for the main data set. This is about ten times lower than in predecessor experiments with ^{76}Ge. The combined energy spectrum of all enriched detectors around the region of interest is shown in Fig. 2. It shows no indication of a peak at $Q_{\beta\beta}$, i.e. the claim of the observation of the $0\nu\beta\beta$-decay in ^{76}Ge is not supported. The limit on the half-life is $T^{0\nu}_{1/2} > 2.1 \times 10^{25}$ yr (90% C.L.) including the systematic uncertainty. A combined analysis of results from the previous experiments with germanium yields $T^{0\nu}_{1/2} > 3.0 \times 10^{25}$ yr (90% C.L.). A global comparison of ^{76}Ge and ^{136}Xe results can be found in the front figure of this chapterwhich provides an even stronger rejection of the claim [1,2,3].

Outlook on phase II: Preparations for Phase II of the experiment are ongoing. GERDA is planned to resume operation in Spring 2014. In Phase II about 20 kg of new enriched BEGe detectors will be added to the detectors of Phase I. The detectors went through an extensive campaign for testing and characterization in the HADES facility, Belgium, and were moved to the Gran Sasso laboratory afterwards. New detector supports and electronics are built to further reduce background and improve detector performance. The detector array will consist of seven strings, and the copper 'mini-shrouds' will be replaced by transparent wave-length shifting shrouds. These allow to read out the argon scintillation light in the vicinity of the detector array with photomultipliers and a surrounding curtain of wavelength shifting fibers coupled to silicon photomultipliers. The light is used to efficiently suppress background events up to three orders of magnitude, as has been demonstrated in the LArGe test facility (liquid argon veto). All in all, Phase II aims to exceed an exposure of 100 kg·yr at a background index of 10^{-3} cts/(keV·kg·yr).

Mark Heisel, K. Tasso Knöpfle, Manfred Lindner, Alexey Lubashevsky

Double Chooz: Reactor Neutrino Oscillations

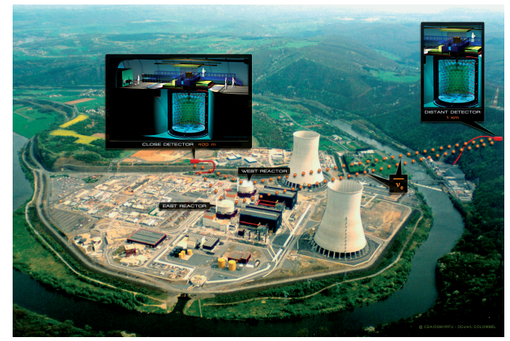

Fig. 3: The Double Chooz configuration.

In the three-neutrino paradigm, the neutrino flavor eigenstates are related to the mass eigenstates through the PMNS mixing matrix, which can be parameterized by three mixing angles and a CP violating phase. Two of the three mixing angles were already known to be large from several solar, atmospheric and reactor neutrino experiments, whereas for the third one, θ_{13}, there were just upper limits for many years. This mixing angle is now measured in Double Chooz. The electron antineutrinos emitted from two nuclear reactors at Chooz, France, are ultimately measured in two detectors. The far detector in 1 km distance from the reactor cores has started data taking in April 2011. It is placed in an underground laboratory providing a rock shielding against cosmic radiation of 330 m w.e.. A second near detector is built at an average distance to the reactors of about 400 m, see Fig. 3. The near detector will measure the neutrino flux without any oscillation effect whereas the far detector is placed near the minimum of the expected oscillation signal. If the electron antineutrinos change their flavor, they are not detected anymore and a reduced electron antineutrino flux is observed for a nonzero value of θ_{13}.

The heart of the Double Chooz detector is about 8.3 tons of a gadolinium-loaded liquid scintillator newly developed at MPIK. In the antineutrino detection reaction protons in this target scintillator are converted into neutrons along with the emission of a positron. The positron created in this inverse beta decay carries the energy information of the neutrino and provides a prompt scintillation light signal in the detector. The neutron produced in the reaction is captured with high probability on the Gd dissolved in the organic liquid within a delay time of some tens of µs. A neutron capture on the Gd creates gamma radiation with a total energy of about 8 MeV. This coincidence signal of a prompt event followed by a delayed event with rather high energy compared to the energies of natural radioimpurities allows efficient background reduction and neutrino signal extraction.

The target scintillator is embedded in an 8 mm thick transparent acrylic vessel which is surrounded by the gamma catcher scintillator with a total mass of 18.1 tons contained in a 12 mm acrylic vessel. Its main purpose is to convert the full energy of the gamma radiation produced in a neutrino interaction into scintillation light. The third volume in the detector is a non-scintillating buffer liquid with a total mass of about 80 tons. It reduces accidental background events created by natural radioactivity coming from outside. The three nested inner volumes are optically separated from the outer detector components by a 3 mm thick cylindrical steel vessel. On the inside of this steel vessel 390 photomultiplier tubes (PMT) are installed. Muons and their spallation products are one of the main sources for background. They are detected in the liquid scintillator of the inner veto, which is around the buffer volume. An additional outer veto system consisting of several sheets of plastic scintillators is installed on top of the detector.

In 2011 the Double Chooz experiment was the first reactor neutrino experiment presenting a hint for a positive value of the neutrino mixing angle θ_{13} [4]. From the first analysis Double Chooz included the shape information of the neutrino energy spectrum to extract the result. In 2012 the Double Chooz result was confirmed with higher precision by the experiments Daya Bay in China and RENO in Korea. In the same year, the Double Chooz analysis was improved with more data and reduced systematics. In this analysis the no-oscillation hypothesis could already be excluded at 99.8 % CL with the Double Chooz far detector only, see Fig. 4 [4]. In

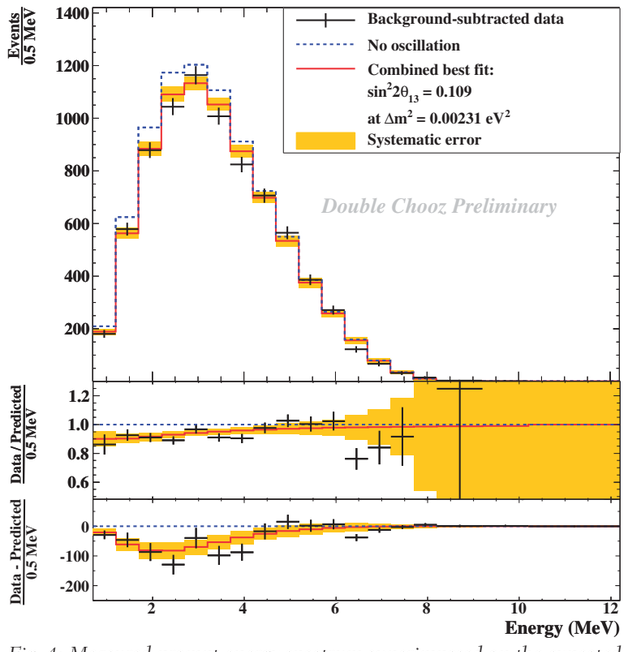

Fig. 4: Measured prompt energy spectrum superimposed on the expected spectrum for the no-oscillation and best fit. The orange band represents the systematic uncertainties on the best-fit prediction.

2013 several cross-check analyses were done demonstrating the robustness of the Double Chooz result. Due to the very low background environment of the Double Chooz detector materials as liquids and PMTs, it was also possible to analyze inverse beta decay events with neutron captures on hydrogen atoms. In this way the fiducial volume of the detector was more than doubled, since the gamma catcher could be included. On the other hand, the signal-to-noise ratio is worse in the H analysis due to the longer coincidence time and the lower energy of the gamma emitted after neutron capture on H (2.2 MeV). The combined Gd and H anaylsis provided the most sensitive DC analysis so far of $\sin^2(2\theta_{13}) = 0.109 \pm 0.035$. With the near detector operational Double Chooz expects to reach a final precision of about 10% (1 sigma) on that value.

An independent analysis based on rate-only information was also performed. Here the observed and expected (in absence of oscillation) neutrino candidate rates are compared for different reactor power conditions, e. g. with both reactors on, one reactor off, both reactors off or intermediate configurations when the reactors are not running at full power. Plotting the observed candidate rate versus the expected rate for these different reactor power conditions allows to fit the data points with a linear model parametrized by θ_{13}. The advantage of this approach is that the analysis is independent of background models. The background is measured directly during both reactor-off periods and added as a data point. This reactor rate modulation analysis was also done for neutron captures on Gd, H and in a combined fit. The result is in very good agreement with the rate and shape result. Besides the main objective of a measurement of the third mixing angle, Double Chooz also performed a Lorentz violation analysis, cosmogenic background research (in particluar during phases with both reactors) off and neutrino directionality studies.

The main hardware contributions from MPIK are the PMTs and the inner detector liquids. The 780 PMTs of the near and far detector were tested and calibrated in a dedicated test rig setup in a light-tight Faraday cage. An accurate calibration of the photomultipliers is a prerequisite for an exact reconstruction of the energy of a neutrino event. Each PMT was characterized with respect to its features like quantum efficiency, quality of the signal and time resolution. All PMTs were successfully installed in the two detectors. The main challenge on the target scintillator side is chemical and optical stability over several years. In the two years of analysed data, in the far detector stable performance on the level of less than 1% per year was found for the energy scale as well as the detection efficiency. The target liquid of the near detector has to be as identical as possible to the one of the far detector. Therefore, the liquid needed for the two detectors was mixed simultaneously beginning of 2010. Half of the Gd scintillator was filled in the far detector and the second half is kept at MPIK until the near detector is filled, which is planned for 2014.

On the simulation and analysis side, the focus of our group was on the modelling of the light production and propagation in the detector, the understanding of the energy scale and studies on the neutron detection efficiency. The Geant4-based detector simulation includes scintillator parameters which are specific for our liquids and were obtained by dedicated measurements in the chemistry laboratory. The main input parameters are light yields, attenuation lengths, emission spectra, reemission probabilities, refractive indices and a lot of quenching parameters. These parameters are varied in the simulation within their uncertainties to match calibration data taken with neutron (^{252}Cf) and gamma sources of different energies.

The key aspects of our data analysis activities are related to energy scale and detector efficiency studies. For the rate and shape analysis a precise knowledge of the energy scale is mandatory. To reach a precision of less than 1% detailed studies of the position dependence of the detector response, energy non-linearity effects and the stability of the energy scale were performed. Besides the data taken with radioactive sources deployed in the central axis of the Double Chooz detector and in several positions of the gamma catcher volume, spallation neutrons captured on H and Gd were used for calibration purposes. So far the Double Chooz result is limited by the knowledge of the antineutrino flux coming from the reactor. This will change as soon as the near detector is finalized. Then it will become very important to reduce the uncertainty on the detection efficiency to the few per mille level. The methods and neutrino candidate selection cuts were optimized to obtain high precision on the fraction of neutrons captured on Gd, the position-dependent inefficiencies due to the energy and time cuts and the influence of boundary effects. These studies pave the ground for an efficient and precise analysis in the important two-detector phase in Double Chooz.

Christian Buck

NUCIFER and STEREO: The Search for Sterile Neutrinos

The radioactive decays of fission products in nuclear reactors produce isotropically emitted electron antineutrinos. Due to the rather high production rate at a localized source, nuclear reactors are well suited for neutrino experiments. The neutrino flux measured in many experiments close to nuclear reactors (distance between detector and reactor <500 m) is lower than the predicted flux rates by more than 6%. The deviation from unity for the observed versus expected neutrino flux ratio has a significance of 2.7 sigma, see Fig. 5. This so-called reactor neutrino anomaly could be explained by oscillations into sterile neutrinos, which are not detected by the experiments. Other possibilities such as so far unknown effects resulting in a common bias in all experiments or additional uncertainties in the theoretical flux calculations are also considered.

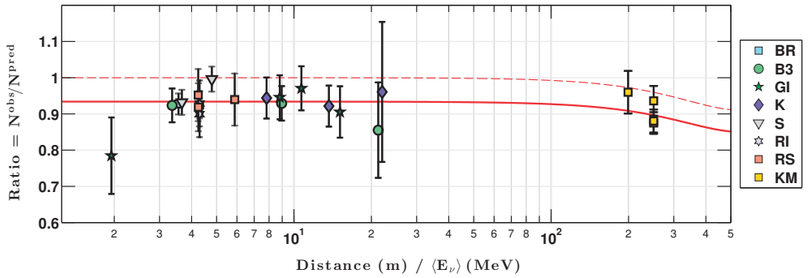

Fig. 5: The reactor neutrino anomaly.

The NUCIFER and STEREO experiments are expected to provide significant input towards a solution of the anomaly. The original goal of the NUCIFER experiment was to investigate whether neutrino detectors could be used for safeguard or non-proliferation applications. An observation of a change in the measured antineutrino spectrum can for example be a hint for the removal of plutonium from the reactor core. The NUCIFER detector is placed at a distance of 7 m from the OSIRIS research reactor (70 MW) at CEA Saclay in France. The detector target consists of 850 liter of a gadolinium-loaded liquid scintillator contained in a cylindrical steel vessel. As in Double Chooz, the neutrinos are detected via the inverse beta decay reaction on hydrogen atoms in the target scintillator, which produces a coincidence signal of a prompt positron event and a delayed neutron capture on a gadolinium atom in the target liquid. The scintillation light is detected by 16 PMTs mounted on the top side of the detector. Between PMTs and the target liquid there is a 25 cm thick acrylic disc. The detector is protected against radiation mainly coming from the reactor by a polyethylene (15 cm) and lead (10 cm) shielding. Finally, the detector is completed by an active veto of 5 cm thick plates of plastic scintillator.

The NUCIFER sensitivity for the search for sterile neutrinos is somewhat limited. The upcoming STEREO experiment is more optimized for this purpose. The detector design of STEREO and NUCIFER is similar, however, the volume of the STEREO target scintillator is more than a factor of two bigger providing more statistics. Moreover, the STEREO target is separated in six cells of equal size. The neutrino source (8 m distance to detector) is a research reactor enriched in ^{235}U with a thermal power of 58 MW (Fig. 6) at the Institute Laue Langevin (ILL) in Grenoble, France. Oscillations into sterile neutrinos would not only be observed by the disappearance of electron antineutrinos, but could also be seen in deformations of the neutrino energy spectrum. There is a slight difference between the distance of each cell to the neutrino source. Therefore, in case of sterile neutrinos, the deformation would be shifted to different energy regions in the reactor neutrino spectrum of each cell.

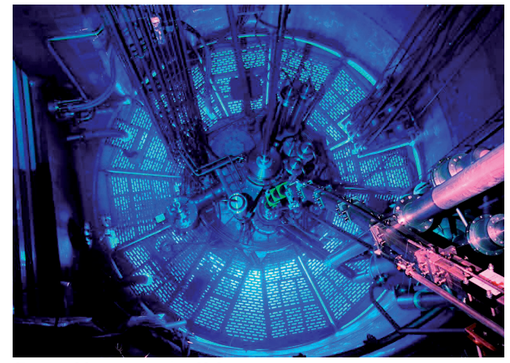

Fig. 6: View into the ILL reactor.

In both experiments the neutrinos are detected in a gadolinium-loaded liquid scintillator (Gd-LS). At MPIK we developed a novel Gd-LS in the context of the Double Chooz experiment. The chemical composition of this organic liquid was modified and optimized for the needs in the NUCIFER and STEREO experiments. The background rate is lowered by a higher Gd concent-

ration reducing the coincidence time of the neutrino signal. Furthermore, the scintillator design was tuned to increase pulse shape discrimination capabilities for further background reduction. As additional detector component, MPIK is also responsible for the PMTs in STEREO. Here we profit from the expertise and infrastructure we have from Double Chooz. This allows us to efficiently test and calibrate the 44 PMTs needed in the detector. The tasks of the MPIK group are completed by a growing involvement in simulation studies and the analysis of experimental data.

Christian Buck

Borexino

Borexino is an experiment aiming at detecting low-energy (<2 MeV) neutrinos from the Sun, the Earth, European nuclear power plants and possibly from core collapse Supernovae in real time and with high statistics. Since May 2007 the Borexino Collaboration consisting of scientists from Italy, the US, Germany, Russia, France, Hungary and Poland has been operating a neutrino detector filled with 300 tons of a liquid scintillator. The scintillation light generated via neutrino or anti-neutrino interactions in the detector is observed by 2212 highly sensitive photomultiplier tubes. The major experimental challenge was given by the necessity to reduce background sources to levels that were never reached before. For this reason, the Borexino detector was built in the Italian Gran Sasso Underground Laboratory, where the overburden of 1.4 km of dolomite rock reduces cosmic radiation by six orders of magnitude. In addition, the onion-like detector was built with materials whose natural radioactivity content decreases from exterior to interior. Finally, at its core a nylon balloon contains the highly radiopure scintillator. Unprecedented radiopurity levels were reached and risky, but necessary internal calibration campaigns did not increase the background.

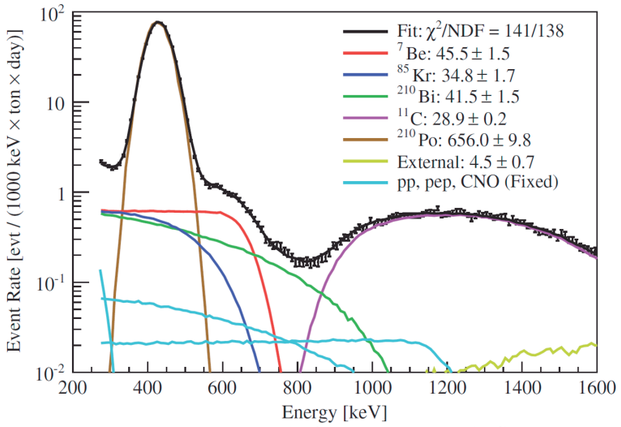

Fig. 7: precision measurement of solar ^{7}Be neutrinos (red) in Borexino including some prominent background components.

Data acquisition was accompanied by a large number of publications in the reporting period (see e. g. [5]). Few of these results are highlighted here. Borexino succeeded in observing individually several sub-branches of the proton-proton fusion reaction chain in the Sun. All measured neutrino rates are consistent with the predictions of the Standard Solar Model and with neutrino oscillations. In particular, Borexino was able to measure the rate from the electron capture of ^{7}Be with 5% precision corresponding to 46 ± 1.5 (stat) ± 1.5 (syst) counts/day/100 tons (see Fig. 7). Moreover, it was possible to determine the rate of neutrinos released in the fusion of two protons with one electron (pep), namely 3.1 ± 0.6 (stat) ± 0.3 (syst) counts/day/100 tons. The latter analysis, which involved a special threefold coincidence method and a novel pulse shape discrimination technique, set also the best upper limit for solar neutrinos emitted in the so-called CNO cycle. Even though it has a marginal role in the Sun's energy release, it is predicted to be the dominating process in hotter and more massive stars, therefore its measurement is important for astrophysical modeling. Finally, Borexino improved its previous result in detecting so-called geo-neutrinos, which are released together with the geothermal energy in U and Th decays in the Earth's interior. For the first time, it was possible to disentangle the contributions from U and Th, and the overall fit agrees very well with most geochemical models of the Earth (see Fig. 8).

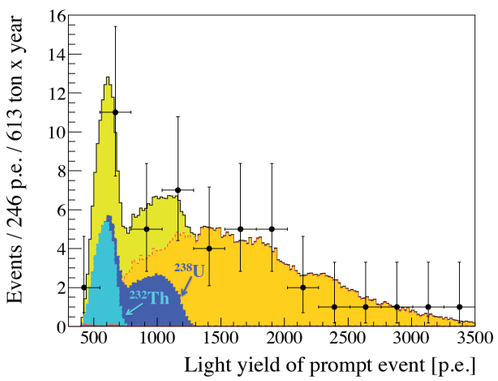

Fig. 8: Spectrum of geo-neutrinos originating from U and Th decays (blue). In orange: neutrino background from European reactors, in yellow: sum.

Werner Maneschg

Theory

The last 15 years saw the emerging of a consistent picture in what regards the phenomenological description of neutrino mass and our knowledge on their parameters. Three tasks are to be addressed, and investigated by the division:

1. Determine the parameters describing neutrino mass and mixing
2. Understand their origin
3. Test for deviations from the standard picture

The group studied for instance formal and phenomenological aspects of the oscillation of neutrinos, in particular in matter, because the extraction of unknown neutrino parameters from future oscillation experiments relies on such matter effects.

In what regards neutrino parameters, global fits of the experimental results were performed, including experiments with solar, atmospheric, reactor and accelerator neutrinos [6] (see Fig. 9). A careful analysis of different data sets can be performed, in order to quantify various hints for certain parameter values. Examples are a non-trivial CP phase, or non-maximal atmospheric neutrino mixing, both of which would have strong theoretical impact. Furthermore, in [7] it was quantified that PINGU, a planned extension of the IceCube neutrino telescope, has the potential to determine the unknown neutrino mass hierarchy, with a timescale (and cost) much below future long-baseline large-scale accelerator experiments. Additional physics potential of PINGU, such as constraining non-standard neutrino physics, was also studied by the group.

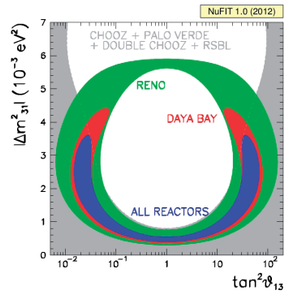

Fig. 9: Allowed regions in the plane of mass-squared difference and mixing angle for different combinations of reactor experiments, from [6].

During the reporting period came a groundbreaking discovery in the form of a non-zero value of the last missing neutrino mixing angle θ_{13}. This result, with other experiments co-discovered by the Double Chooz experiment, that has strong MPIK contribution, started a huge worldwide model building activity. Before the discovery, essentially all models were constructed to generate $\theta_{13}=0$. The phenomenological and theoretical implications of a non-zero value finding were studied by the group with various approaches and methods. One example for the phenomenology is that the large value of θ_{13} implies a lower limit on the branching ratio of the decay $\mu \rightarrow e\gamma$, in very natural scenarios of New Physics („minimal flavor violation"). With the measured value of θ_{13}, the decay is guaranteed. This illustrates that results in neutrino physics imply important consequences for other fields of high-energy physics.

In what regards models, the straightforward Ansatz is to introduce flavor symmetries, typically based on discrete non-Abelian groups. Several methods were followed. For instance, one can note that flavor symmetry models typically end up in having subgroups of the original symmetry group as residual symmetries of the neutrino and charged lepton mass matrices. This allows for a scan of all discrete groups up to a certain order with modern computer algebra programs. New lepton mixing schemes can be found in this way.

Another idea is to combine the flavor symmetry with the CP symmetry. This predicts the leptonic CP phase and has potential impact on the baryon asymmetry of the Universe. Here concrete models were constructed in the division, as well as formal mathematical consistency aspects to combine the different operations of CP and flavor symmetry clarified.

A completely different idea to approach neutrino mixing is to use Abelian U(1) symmetries. This connects flavor and gauge symmetries, a unique situation. The resulting models are less predictive, but contain much less new parameters and particles than the discrete non-Abelian flavor symmetry models. If the U(1) is broken at a not too high energy scale, then rich phenomenology is however still possible: the gauge boson mixes with the Z-boson of the SM, can lead to lepton flavor violation, or explain the magnetic moment of the muon.

Apart from the peculiar mixing pattern of neutrinos, the smallness of neutrino mass is the second big question to be answered. The seesaw mechanism, introducing fermion singlets that couple to each other, as well as to leptons and the Higgs particle, is here the most popular candidate. Formal aspects to parametrize the unknown parameters contained in the seesaw framework were discussed, as well as variants of the standard seesaw. The interaction of singlets with leptons and the Higgs particle can influence the interpretation of that recently discovered particle. In the minimal SM, the electroweak vacuum seems to be metastable, which means that our Universe may eventually go through a phase transition to the true minimum. The singlet-lepton-Higgs vertex influences the evolution of the Higgs self-coupling, which now runs towards more negative values than without the seesaw mechanism. Therefore, the electroweak vacuum is instable, i. e. the vacuum will surely go to a more minimal state than it is currently in: therefore, something must replace the SM + seesaw model!

Moreover, if one of the fermion singlets has masses in the regime of keV, then it can be a Warm Dark Matter (WDM) particle. While Cold Dark Matter (CDM) is the most often candidate for dark matter, WDM can solve some of the problems of the CDM paradigm, for instance the too low number of dwarf galaxies. The division has presented new ways to generate the Dark Matter density in gauge extensions of the SM, and discussed possibilities to bring the mass of the singlets down to keV. One example is to apply broken flavor symmetries, which in the unbroken limit predict one massless neutrino. Another example takes advantage of the so-called Froggatt-Nielsen mechanism, which is typically present to explain the mass hierarchy of the charged leptons, but was noted to be applicable to the fermion singlets as well, thereby allowing to consistently describe fermion mass and mixing, as well as WDM.

As mentioned, there are many scenarios that lead to massive Majorana neutrinos. All have in common that they predict lepton number violation. Therefore, neutrinoless double beta decay is expected to be present at some level. Here the division was involved in studying the theoretical interpretation of a possible detection of the decay. In addition, the importance of different nuclear physics calculation of the lifetime was emphasized [8]. This is especially important when the results on double beta decay from different isotopes are compared. In fact, the GERDA collaboration has used this result in the analysis of the limit that they obtained.

The division has also studied non-standard neutrino physics, in particular light sterile neutrinos. A variety of hints in particle and astroparticle physics (most recently the „reactor anomaly"), as well as cosmology, points towards the existence of sterile neutrinos, having mass of order eV and mixing of order 0.1 with the SM fermions. The division was involved in global fits that support the various hints, as well as models, which explain the existence of the light sterile neutrinos in a variety of scenarios. In general, sterile neutrinos can have arbitrary masses, and aspects of different cases, e. g. MeV or TeV, in order to explain certain experimental discrepancies such as the invisible Z-decay width, were also studied.

Manfred Lindner, Werner Rodejohann

The GIOVE Gamma-Ray Spectrometer

The GIOVE (Germanium Inner Outer Veto, see Fig. 10) gamma-ray spectrometer, designed for very weak radioactivity measurements, has been completed in 2012 at the MPIK low-level underground laboratory (LLL – shielded by 15 meters of water equivalent). Its excellent background performance due to a novel passive and active shielding concept allows for sensitivities close to those of the GeMPI spectrometers, which are operated at the Gran Sasso Underground Laboratory underneath about 250 times more overburden. The double veto system in addition to several neutron moderation layers results in a suppression factor close to 100 for the muon-induced background component, compared to 11 – 14 for the former low-background gamma-ray spectrometers at the LLL. Further progress was also made in ^{222}Rn suppression prior to starting the actual counting measurement, which can save up to weeks of screening time. The sample is enclosed in an air-tight copper container, flushed with nitrogen and is stored (before counting) inside the Rn-free glove-box system of GIOVE until ^{226}Ra/^{222}Rn equilibrium is reached.

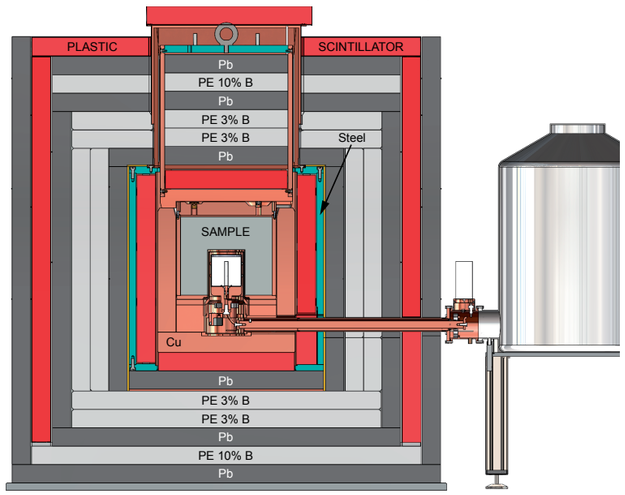

Fig. 10: Sketch of the GIOVE gamma-ray spectrometer showing the active and passive shielding layers.

Monte-Carlo simulations of the full detector-source setup have been performed in order to characterize precisely the active volume of the crystal, and to evaluate the counting efficiency for any sample geometry. The complete shield is implemented in a Geant4-based framework, so that residual background contributions can be investigated.

GIOVE participates in the screening of materials for low radioactivity concentrations to be used in the double-beta-decay experiment GERDA phase II, the Dark-Matter experiment XENON1T and other low-background projects. It proves that highly sensitive gamma spectrometry at the range of 100 µBq/kg can be achieved even at shallow depth of the home-based laboratory with its immediate accessibility [n].

Gerd Heusser, Marc Weber

Detection of ^{133}Xe from the Fukushima Nuclear Power Plant in the Upper Troposphere above Germany

After the accident in the Japanese Fukushima Dai-ichi nuclear power plant in March 2011, large amounts of radioactive gases were ejected and distributed in the atmosphere. Such a strong release opens up the possibility to probe global atmospheric circulation models using ^{133}Xe as a tracer. In a collaboration with the DLR (Deutsches Zentrum für Luft und Raumfahrt) we collected worldwide unique air samples from various altitudes and places above Germany.

The detection of ^{133}Xe isotope traces in small (liter-scale) samples was only possible by combining miniaturized ultralow-background proportional counters developed at MPIK for the GALLEX experiment with knowledge acquired during Dark-Matter searches with liquid xenon (XENON100 and XENON1T). The measurements were performed with a chromatographic xenon extraction procedure followed by low-background counting of ^{133}Xe β-decays in a dedicated counting setup with passive and active shielding in MPIK's underground laboratory.

With this technique a detection limit of the order of 100 ^{133}Xe atoms in liter-scale air samples corresponding to an activity of about 100 mBq/m^3 was achieved. In total six samples from two research flights on March, 23 and April, 14 were analyzed. In five of them ^{133}Xe traces above the detection limit could be detected [10]. Our results reveal that in comparison to the ground-based measurements by the Bundesamt für Strahlenschutz, the ^{133}Xe plume arrived several days earlier at high altitudes in Germany. They also proof that ^{133}Xe-enriched ground-level air masses from the Japanese region were lifted to the upper troposphere where fast high-altitude winds accelerate their global transport. The atmospheric aspects of the ^{133}Xe data as well as the interpretation of simultaneously measured trace gases and aerosols is topic of a second paper under preparation.

Ludwig Rauch, Hardy Simgen

References:

[1] K. H. Ackermann et al. [GERDA Collaboration], Eur. Phys. J. C 73 (2013) 2330.
[2] M. Agostini et al. [GERDA Collaboration], arXiv:1306.5084 and Eur. Phys. J. C 73 (2013) 2583.
[3] M. Agostini et al. [GERDA Collaboration], Phys. Rev. Lett. 111 (2013) 122503.
[4] Y. Abe et al. [Double Chooz Collaboration], Phys. Rev. Lett. 108 (2012) 131801 and Phys. Rev. D 86 (2012) 052008.
[5] G. Bellini et al. [Borexino Collaboration], Phys. Rev. Lett. 107 (2011) 141302 and Phys. Rev. Lett. 108 (2012) 051302 and Phys. Lett. B 722 (2013) 295-300.
[6] M. C. Gonzalez-Garcia, M. Maltoni, J. Salvado and T. Schwetz, JHEP 2012(12).
[7] E. K. Akhmedov, S. Razzaque and A. Y. Smirnov, JHEP, 2013(02), 1-39.
[8] P. S. Bhupal Dev, S. Goswami, M. Mitra and W. Rodejohann, Phys. Rev. D 88 (2013) 091301.
[9] G. Heusser et al., AIP Conf. Proc. 1549 (2013) 12-15.
[10] H. Simgen et al, arxiv:1309.1618.

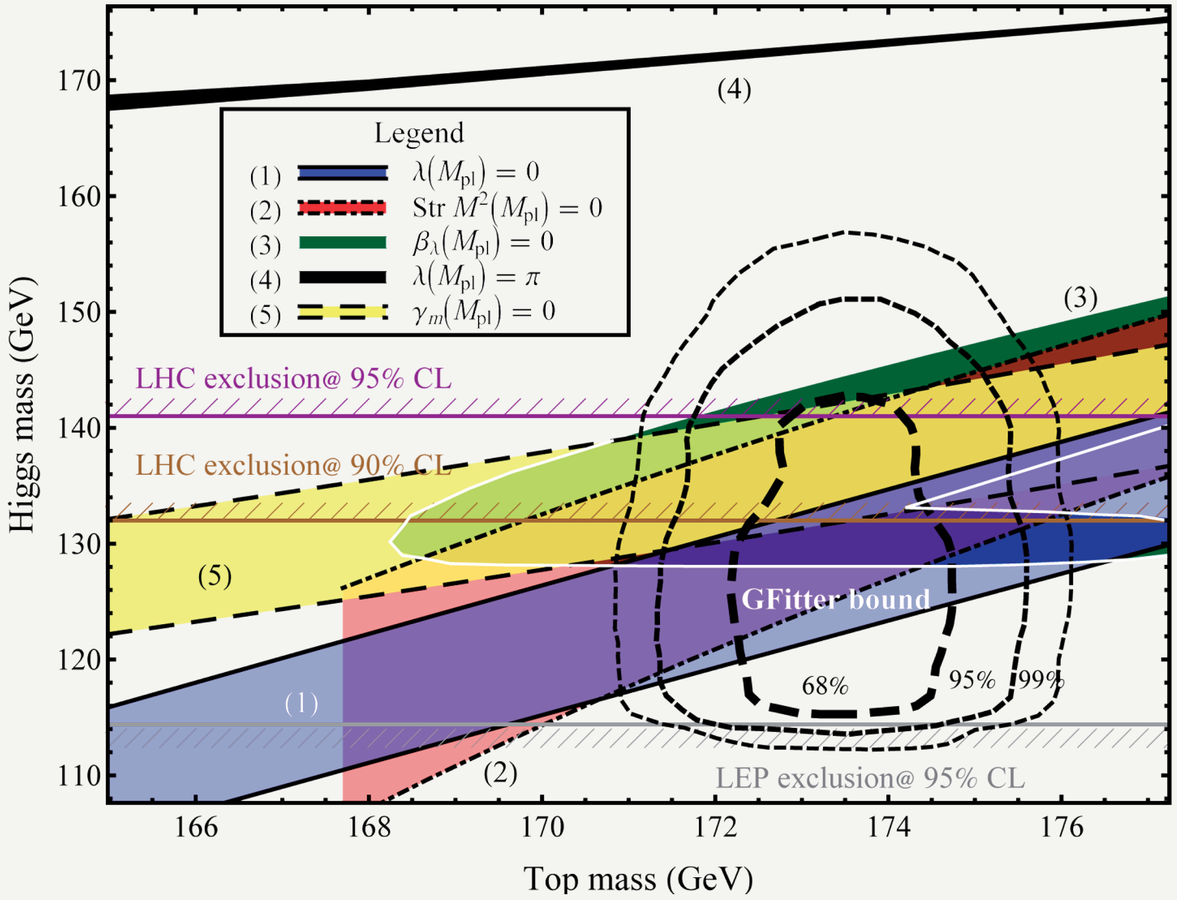

Higgs and top mass values from different theoretical boundary conditions (see insert) at the Planck scale [1] before the discovery of the Higgs particle. Shown is also the experimental situation at that time: The gray-hatched line at the bottom was the lower bound from LEP. The purple (brown) lines indicate the LHC Higgs upper bounds from the 2010 data and the black dashed lines show the electroweak precision fit. Meanwhile the Higgs and top mass are known to be 125.9 ± 0.4 and 173.2 ± 0.9 GeV, respectively, which matches very well.

1.5 Physics beyond the Standard Model

Introduction

The Standard Model (SM) of particle physics is very successful in describing subatomic physics. A number of experimental and theoretical reasons are, however, known which strongly point to the fact that the SM is incomplete and that at some higher energy it must be embedded into some new theory. The experimental facts beyond the SM are finite neutrino masses, the baryon asymmetry of the Universe and the existence of Dark Matter. On the theory side there exists in addition a whole list of arguments pointing in the same direction. Various aspects concerning new physics beyond the SM were therefore studied in the reporting period.

The Higgs Mass and the Hierarchy Problem

Significant progress in understanding the SM and its possible extension has been achieved in the last two years, driven in particular by the discovery of the Higgs boson in 2012. The existence of this scalar particle completes the SM, but also triggers many fundamental questions on its properties. The vacuum expectation value of the SM Higgs field generates masses for all the elementary particles we have observed so far. However, its own mass is quadratically sensitive to the mass scale of new physics that it couples to, which could be orders of magnitude larger than its natural value. Such a precise tuning of the Higgs boson mass, known as the "hierarchy problem", is puzzling and indicates that physics beyond the SM that protects the Higgs mass against large quantum corrections should exist in the multi-TeV regime. We investigated several approaches to solving the hierarchy problem, such as supersymmetry (SUSY) and conformal symmetry.

Before the discovery of the Higgs boson, bounds on its mass were obtained by examining the theoretical constraints on the SM, such as triviality and vacuum stability. The SM can survive up to the Planck scale provided that the mass of Higgs boson is between 125 and 180 GeV. With the help of the renormalization group equations we have studied the possible Planck scale boundary conditions [1] that set the mass for the Higgs particle, with some of the possibilities close to the value measured at the LHC. The Higgs particle that has been discovered at CERN is a CP-even scalar boson and could be the first truly fundamental scalar particle observed in nature. The discovery of the Higgs boson also provides a new portal to search for new physics such as flavor violating Higgs coupling to leptons and quarks [2], the possible existence of more than one Higgs particle, of extra dimensions, or of new composite dynamics (see Fig. 1).

One of the possible candidates to solve the hierarchy problem is supersymmetry, which unifies bosons and fermions into one complete framework, shielding the scalar boson mass from high-

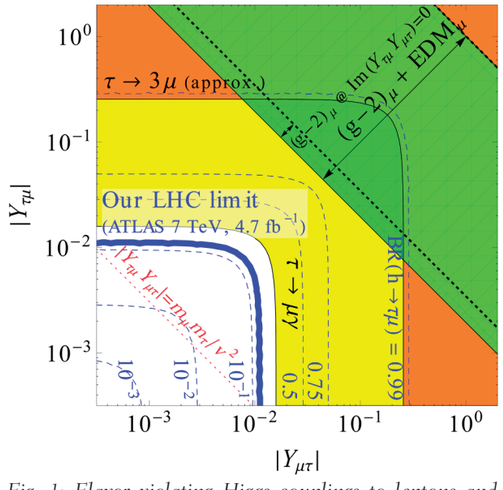

Fig. 1: Flavor violating Higgs couplings to leptons and quarks are especially interesting probes of new physics, since they can arise in many frameworks of new physics at the electro-weak scale, such as two Higgs doublet models, extra dimensions, or models of compositeness. The plot shows constraints on the flavor violating Yukawa couplings $|Y_{\mu\tau}|$ and $|Y_{\tau\mu}|$ resulting from various experimental inputs.

energy correction. SUSY requires essentially the doubling of the particle content compared to the SM, with the lightest superpartner (typically a so-called "neutralino") providing a natural candidate for Dark Matter. Using the latest result from LHC, XENON100 and cosmology as input, the level of fine-tuning of neutralino Dark Matter was investigated in the low-energy phenomenological minimal supersymmetric SM, ruling out a large fraction of the un-tuned parameter space (see section 1.3). This has theoretical implications, since in the generic minimal supersymmetric model it is difficult to understand the observed Higgs mass without fine-tuning. It is therefore interesting to consider extensions of the minimal model such as the next-to-minimal supersymmetric SM or the adjoint minimal supersymmetric SM [3] which can ameliorate such difficulties. Other possibilities such as R-parity violation, which could dramatically change the collider phenomenology of supersymmetric particles, were also studied.

Kher Sham Lim, Manfred Lindner

Unification

SUSY also provides strong support for the hypothesis of Grand Unification of fundamental gauge forces at high energies, around 10^{16} GeV. On the other hand, if all gauge couplings are unified at such a high energy scale, it is puzzling that no new physics should exist between the SUSY scale and the Grand Unification scale. Also, Grand Unification typically predicts proton decay due to baryon number violating operators. In the SM, baryon (B) and lepton (L) number are accidental global symmetries of the renormalizable couplings. These symmetries can be promoted to gauge symmetries that are spontaneously broken. Theoretical inconsistencies – so-called anomalies – that might arise in this case, can be resolved if leptoquarks, i. e., fields that carry both B and L, are introduced. A specific model of this type, consistent with collider bounds and cosmology, has been considered in [4]. The model also contains a fermionic Dark Matter (DM) candidate, whose stability is a direct consequence of the breaking of the gauged B and L symmetries. Unlike in many other DM models, there is thus no need to impose an extra discrete symmetry. If only B, but not L, is promoted to a gauge symmetry, one can construct a simple DM model that contains only four free parameters and is therefore fully testable in the future by combining DM and collider experiments which was shown in other publications. In models that possess a left-right (parity) symmetry, the spontaneous breaking of B and L can be related to the spontanous breakdown of parity. In a minimal model of this type, the leptoquark fields that are necessary for anomaly cancellation have the additional benefit of generating neutrino masses via the type III seesaw mechanism. Additionally, this theory predicts the existence of two light sterile neutrinos. In all these setups, the local B and L symmetries can be broken at a scale close to the electroweak scale, while maintaining consistency with experimental constraints on baryon number violating processes like proton decay.

Michael Dürr, Pavel Fileviez Perez

Conformal Symmetry

The usual theoretical extensions of the SM require the existence of new particles with masses around the TeV scale in order to solve the hierarchy problem and to avoid unacceptable fine-tuning. The absence of fine-tuning is often referred to as "naturalness" of a theory. But so far there is up to energies of about ~2 TeV absolutely no sign of new physics beyond the SM at the LHC and other experiments. Therefore, the logic behind the long-standing theoretical paradigm of naturalness has to be reexamined. One possible class of theories that could explain the absence of new particles while still providing a solution to the hierarchy problem is connected to conformal symmetry, where no mass scales are explicitly introduced in the Lagrangian. The electro-weak scale would be generated by quantum effects possibly induced at very high mass scales by quantum gravity and the scale separation would be protected by the residual effects of conformal symmetry. The crucial assumption for this mechanism to work is that there is no new physics scale between the electroweak scale and the Planck scale at ~ 10^{19} GeV. However, there should be some new physics connected to the electro-weak scale which leads to Dark Matter candidates and which

explains neutrino masses. A specific model with a new hidden sector (i. e. an extra gauge factor) and new particles in this hidden sector was considered. There exist new interactions in the hidden sector similar to quantum chromodynamics (QCD), but this sector communicates only very weakly with SM particles. In this theory, the renormalization group running of the coupling in this new sector generates the electro-weak scale dynamically through spontaneous breaking of chiral symmetries in the hidden sector. As a consequence of this chiral symmetry breakdown one obtains condensates of new fermions leading also to electro-weak symmetry breaking in the SM sector. The model looks therefore at low energies as far as it is tested fully like the SM and it provides via the hidden sector good Dark Matter candidates [5].

Martin Holthausen, Kher Sham Lim, Manfred Lindner

The Baryon Asymmetry of the Universe

An open issue in cosmology is the baryon asymmetry of the Universe, i. e., the question why the Universe consists predominantly of matter, with virtually no antimatter. This asymmetry can only be understood in theories that violate baryon number and CP (particle-antiparticle) symmetry, and in which the Universe evolves far from thermal equilibrium during part of its early life. One possible mechanism of this type is leptogenesis, where CP-violating decays of heavy neutrino species in the early universe generate a lepton number asymmetry, that is later converted into a baryon number asymmetry. A precise calculation of heavy neutrino decays far from thermal equilibrium requires methods of non-perturbative quantum field theory, which have been developed and studied extensively in our group [6]. A particularly appealing model of leptogenesis that has been investigated is the neutrino-minimal Standard Model (νMSM) [7], which explains not only the baryon asymmetry of the Universe, but also Dark Matter, neutrino masses and neutrino oscillation in a coherent framework.

Daniel Schmidt

Higgs Portal Connection to Dark Matter

Cosmological observations have verified that 84.5% of the matter content of the Universe is formed by a non-baryonic, not electromagnetically interacting kind of particle matter, the so called Dark Matter. It is interesting to study what the possible connections between this Dark Matter and the Standard Model content are and if it is possible to solve outstanding problems of the Standard Model, e. g., neutrino physics, by means of the DM connection.

The recently confirmed Higgs sector could involve further Higgs particles which only interact with the Dark Matter. However, Higgs mixing generates a portal between the DM and the Standard Model, which can produce the DM relic density and make Dark Matter direct detection possible, see Fig. 2. The Higgs portal was studied in the context of spontaneous symmetry breaking due to a new Higgs particle [8]. Neutrino masses and a mass for the Dark Matter are then given by the vacuum expectation value of that Higgs particle.

Daniel Schmidt

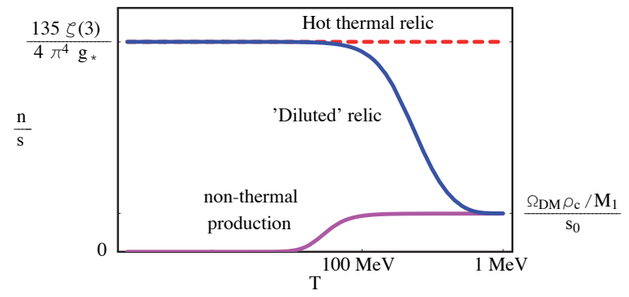

Fig. 2: Schematic evolution of the relic abundance in a scenario with keV sterile neutrino Dark Matter in the Universe. The dashed line is a thermal relic decoupled while being relativistic (hot thermal relic), leading to the overclosure of the Universe. The blue decreasing line is the same hot thermal relic, but with the abundance diluted by rapid expansion of the Universe (entropy production), leading to correct DM abundance. The magenta line depicts the evolution of the nonthermally produced particle with zero primordial abundance.

Predictive Dark Matter with Gauge Kinetic Mixing

In asymmetric Dark Matter models, the DM relic density is explained by an asymmetry between Dark Matter and Dark Antimatter. Such an asymmetry can be fully determined by the measured baryon asymmetry. Consequently we can expect a predictive DM mass, making possible concrete statements on DM. The mirror world, which has an $SU(3)'_c \times SU(2)'_L \times U(1)'_Y$ dark sector parallel to the ordinary $SU(3)_c \times SU(2)_L \times U(1)_Y$ sector, is an attractive asymmetric Dark Matter scenario. A class of mirror models was proposed in order to show that the baryonic and Dark Matter asymmetries can have a common origin with the neutrino masses. In such models the U(1) kinetic mixing can mediate testable Dark Matter scattering. If a mirror discrete symmetry is further imposed, our models will not require more unknown parameters than the traditional type-I, type-II or type-I+II seesaw models for Majorana neutrinos.

Apart from the mirror world scenario, one could think of a dark parity extension of the ordinary electroweak theory. In the $SU(3)_c \times [SU(2)_L \times U(1)_Y] \times [SU(2)'_R \times U(1)'_Y]$ context, it was demonstrated that the dark electron can remain stable while other dark particles can decay fast. The dark electron can annihilate into the dark photon and then obtain a relic density. This relic density will only depend on the dark electron mass since the parity symmetry identifies the dark gauge couplings to the ordinary ones. So, the dark electron should have a predictive mass about 302 GeV if it is the Dark Matter particle. In the presence of a U(1) kinetic mixing, our Dark Matter particle can be verified by DM direct detection experiments. For details see e. g. [9].

Pei-Hong Gu

Possible Connection between Dark Matter and Neutrino Physics

The nature of Dark Matter is excellently described by new particle species which are stable, neutral and non-baryonic. Such a "gauge-singlet" particle is also useful to make neutrinos massive. It is thus interesting to speculate that the neutrino mass and Dark Matter might share the same origin. In Ref. [10] this idea was implemented in a concrete model and demonstrated that neutrino mass and Dark Matter can indeed originate from a common sector beyond the Standard Model. It was assumed that the particles belonging to this new sector feel a new force other than the well-known strong, weak, and electromagnetic forces. If this force turns to a short-range force from a long-range one – just like the weak force – due to the phase transition taking place when the temperature of the Universe is around TeV, a Dark Matter mass of order 100 GeV and the observed small neutrino masses ($\sim 10^{-3}$ to 10^{-2} eV) are both naturally obtained. The DM candidate becomes stable because of the symmetry associated with the new force. The neutrino masses are suppressed since the ordinary neutrinos do not feel this new force at the classical level, so that the neutrino masses show up at some quantum loop level. Possible signatures of such scenarios in experiments, especially at the LHC and other future colliders, as well as direct detection experiments of Dark Matter were studied.

Atsushi Watanabe

Other Topics

Many other theoretical topics were studied in the reporting period which can not be covered here due to space limitations. Examples are models of leptogenesis, specific flavour symmetries and lepton number violation. Various Dark Matter scenarios like asymmetric Dark Matter, warm Dark Matter, inelastic Dark Matter, fermionic Dark Matter were also studied. Other topics include quantum field theoretic description of neutrino oscillations, Lorentz invariance violation and theoretical questions connected to cosmology.

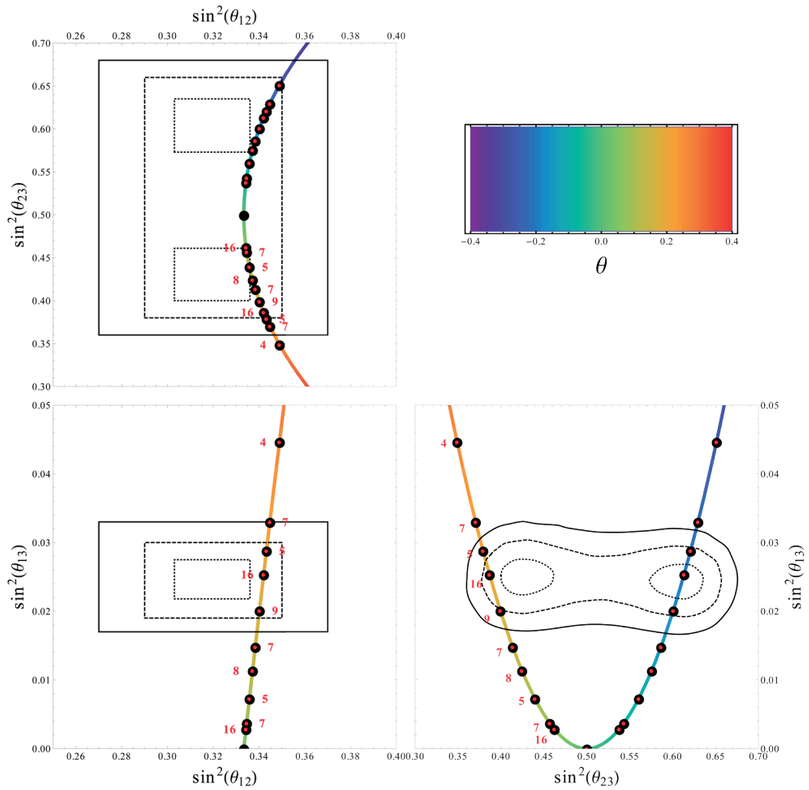

Fig. 3: Regularities in the quark and lepton mixing angles might be explained by flavour symmetries. The plot shows predictions for leptonic mixing angles from a scan of over one million discrete groups up to order 1536. Only a few groups can explain the experimental values and it can also be seen that the predictions fall on lines and do not cover the full parameter plane.

References:

[1] M. Holthausen, K. S. Lim and M. Lindner, JHEP 1202 (2012) 037.
[2] R. Harnik, J. Kopp and J. Zupan, JHEP 1303 (2013) 026.
[3] P. Fileviez Perez and S. Spinner, Phys. Lett. B723 (2013) 371-383.
[4] M. Duerr, P. Fileviez Perez and M. B. Wise, Phys. Rev. Lett. 110 (2013) 231801.
[5] M. Holthausen, J. Kubo, K. S. Lim and M. Lindner, JHEP 1312 (2013) 076.
[6] T. Frossard et al. Phys. Rev. D87 (2013) 085009.
[7] L. Canetti, M. Drewes, T. Frossard and M. Shaposhnikov, Phys. Rev. D87 (2013) 093006.
[8] M. Lindner, D. Schmidt and T. Schwetz, Phys. Lett. B 705 (2011) 324.
[9] P. H. Gu, Nucl. Phys. B872, 38 (2013) and arXiv:1304.7647.
[10] M. Lindner, D. Schmidt and A. Watanabe, arXiv:1310.6582.